

# Taxonomy of asteroid families among the Jupiter Trojans: Comparison between spectroscopic data and the Sloan Digital Sky Survey colors

F. Roig<sup>1</sup>, A. O. Ribeiro<sup>1</sup>, and R. Gil-Hutton<sup>2</sup>

<sup>1</sup> Observatório Nacional, Rua Gal. José Cristino 77, Rio de Janeiro, 20921-400, Brazil

<sup>2</sup> Complejo Astronómico El Leoncito (CASLEO) and Univ. Nacional de San Juan, Av. España 1512 sur, San Juan, J5402DSP, Argentina

Received / Accepted

## Abstract

*Aims.* We present a comparative analysis of the spectral slope and color distributions of Jupiter Trojans, with particular attention to asteroid families. We use a sample of data from the Moving Object Catalogue of the Sloan Digital Sky Survey, together with spectra obtained from several surveys.

*Methods.* A first sample of 349 observations, corresponding to 250 Trojan asteroids, were extracted from the Sloan Digital Sky Survey, and we also extracted from the literature a second sample of 91 spectra, corresponding to 71 Trojans. The spectral slopes were computed by means of a least-squares fit to a straight line of the fluxes obtained from the Sloan observations in the first sample, and of the rebinned spectra in the second sample. In both cases the reflectance fluxes/spectra were renormalized to 1 at 6230 Å.

*Results.* We found that the distribution of spectral slopes among Trojan asteroids shows a bimodality. About 2/3 of the objects have reddish slopes compatible with D-type asteroids, while the remaining bodies show less reddish colors compatible with the P-type and C-type classifications. The members of asteroid families also show a bimodal distribution with a very slight predominance of D-type asteroids, but the background is clearly dominated by the D-types. The L4 and L5 swarms show different distributions of spectral slopes, and bimodality is only observed in L4. These differences can be attributed to the asteroid families since the background asteroids show the same slope distributions in both swarms. The analysis of individual families indicates that the families in L5 are taxonomically homogeneous, but in L4 they show a mixture of taxonomic types. We discuss a few scenarios that might help to interpret these results.

**Key words.** Minor planets, asteroids

## 1. Introduction

Trojan asteroids are a very interesting population of minor bodies due to their dynamical characteristics and physical properties. The main hypotheses about the origin of the Jupiter Trojans assumed that they formed either during the final stages of the planetary formation (Marzari & Scholl 1998), or during the epoch of planetary migration (Morbidelli et al. 2005), in any case more than 3.8 Gy. ago. The dynamical configuration kept the Trojans isolated from the asteroid Main Belt throughout the Solar System history. In spite of eventual interactions with other populations of minor bodies like the Hildas, the Jupiter family comets, and the Centaurs, their collisional evolution has been dictated mostly by the intrapopulation collisions (Marzari et al. 1996, 1997). Therefore, the Jupiter Trojans may be considered primordial bodies, whose dynamical and physical properties can provide important clues about the environment of planetary formation.

Several studies have addressed the dynamical properties of the Trojan population. Of particular interest for the present work are the papers by Milani (1993) and Beaugé & Roig (2001), who computed proper elements for a large number of Jupiter Trojans and realized the existence of several dynamical families. These

authors found that the families are mostly concentrated at the L4 swarm, and they are much less conspicuous at the L5 swarm.

On the other hand, spectrophotometry has been used by different authors to provide information about the surface physical properties of the Jupiter Trojans. Zellner et al. (1985) provided the first multiband photometric observations of 21 of these objects. This allowed to classify them within the D and P taxonomic classes (Tholen 1989), with a significant predominance of the D class (about 90% of bodies). Jewitt & Luu (1990) obtained spectra in the visible range of 32 Trojans and concluded that they show significant analogies with the spectra of cometary nuclei. Eighteen Trojan asteroids have been observed in the framework of the two major spectroscopic surveys: the SMASS (Xu et al. 1995; Bus & Binzel 2002) and the S3OS2 (Lazzaro et al. 2004). Analyzing data from this latter survey, Carvano et al. (2003) concluded that Trojan spectra show differences in spectral slope with respect to the population of D type asteroids in the main belt. Specific surveys have also contributed to increase the spectral data of Jupiter Trojans in the visible. In particular, Bendjoya et al. (2004) observed 34 Jupiter Trojans, while Fornasier et al. (2004) studied 26 asteroids, most of them members of asteroid families detected in the L5 swarm. Spectra in the near infrared (NIR) have been obtained by Luu et al. (1994), and more recently by Dotto et al. (2006) and by Fornasier et al. (2007) who provide photometric colors and spectra both in the visible and NIR of 54 asteroids

that are members of the main asteroid families in L4 and L5. Surface mineralogy based on NIR spectra has been analyzed by Emery & Brown (2003), and recently by Yang & Jewitt (2007) who addressed the presence of water ice on the Trojan surfaces. A very complete analysis of the properties of Jupiter Trojans observed by the Sloan Digital Sky Survey (SDSS) has been developed by Szabó et al. (2007), who addressed an interesting correlation between colors and orbital inclinations. All these studies indicate that Jupiter Trojans seem to be a quite homogeneous population in terms of taxonomy and surface mineralogy.

In spite of these works, the amount of spectroscopic data of Jupiter Trojans presently available is still small to allow a statistical analysis of the taxonomic properties of these bodies. Moreover, since spectra come from different sources they do not constitute a homogeneous data sample. In this paper, we analyze the taxonomy of Jupiter Trojans using data contained in the 3rd release of the SDSS Moving Objects Catalog (MOC3), and compare the results to the available spectroscopic data, *with particular emphasis on Trojan asteroid families*. The SDSS-MOC3 colors have proved to be a very useful tool to characterize the taxonomy of Main Belt asteroids, as recently addressed by Roig & Gil-Hutton (2006), Binzel et al. (2006, 2007), Duffard & Roig (2007), Roig et al. (2007), Gil-Hutton & Brunini (2007), and Hammergren et al. (2007). The paper is organized as follows: Section 2 introduces the two data samples used in this study and compares their internal accuracy. Section 3 is devoted to the global analysis of the color and taxonomy distributions of the data samples. Section 4 concentrates on the particular analysis of selected asteroid families. Finally, Section 5 contains the conclusions.

## 2. Selection of the data samples

In this work, we will analyze two different data sets containing information on Trojan asteroids taxonomy. They are described in the following.

### 2.1. The Sloan sample

The first data set is constituted by observations from the SDSS-MOC3 and their selection required some care. The SDSS-MOC3 includes photometric measurements of more than 204 000 moving objects, of which only 67 637 observations have been effectively linked to 43 424 unique known asteroids. The observations consist of calibrated magnitudes in the  $u, g, r, i, z$  system of filters, centered at 3540, 4770, 6230, 7630 and 9130 Å, respectively, and with bandwidths  $\sim 100$  Å (Fukugita et al. 1996). We adopted here a procedure similar to that of Roig & Gil-Hutton (2006). First, we used the solar colors provided by Ivezić et al. (2001) to compute the reflectance fluxes  $F_v$  in the five bands, normalized to 1 at the  $r$  band. Then, we discarded the observations with error  $> 10\%$  in any of the  $F_g, F_r, F_i$  and  $F_z$  fluxes. Observations showing anomalous values of the fluxes, like  $F_u > 1.0$ ,  $F_g > 1.3$ ,  $F_i > 1.5$ ,  $F_z > 1.7$ , and  $F_g < 0.6$  were also discarded. Note that the error in  $F_u$  has not been constrained, which allows to get a final data set with more than twice the amount of observations than if we restrict this error to be less than 10%. As we will explain later, this error is not critical for our study.

We ended up with a sample of 40 863 observations corresponding to 28 910 unique known asteroids. The distribution of these observations in the space of principal components is shown in Fig. 1 (gray dots), where the first and second principal components,  $PC_1$  and  $PC_2$ , have been computed from the reflectance

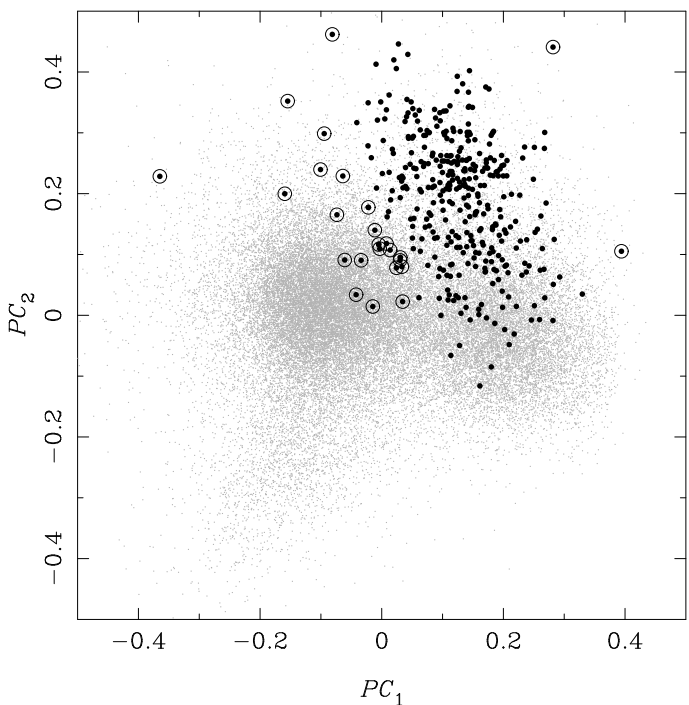


**Figure 1.** Distribution of 40 863 observations selected from the SDSS-MOC3 (gray dots) in the space of first and second principal components. The black dots correspond to 371 observations of known Jupiter Trojans, but those surrounded by a circle have been discarded (see text).

fluxes as:

$$PC_1 = 0.886F_u + 0.416F_g - 0.175F_i + 0.099F_z - 0.849$$

$$PC_2 = -0.049F_u - 0.003F_g + 0.284F_i + 0.957F_z - 1.261$$

The use of principal components allows an easy interpretation of the observations in a bidimensional space. Observations with  $PC_1 \gtrsim 0$  correspond to featureless spectra (e.g. C-, X- and D-type asteroids), while those with  $PC_1 \lesssim 0$  correspond to featured spectra that show a broad absorption band longwards of 7000 Å (e.g. S- and V-type asteroids). The value of  $PC_2$  is related to the overall slope of the spectrum, the larger the  $PC_2$  the higher the slope. For featureless spectra,  $PC_2$  gives an idea of how reddish is the spectrum; for featured spectra, it gives an idea of the band depth (see Roig & Gil-Hutton 2006).

Within these 40 863 observations, we identified 371 observations corresponding to 257 different Trojan asteroids listed in the database of Trojan proper elements maintained by the PETrA Project (Beaugé & Roig 2001; <http://staff.on.br/froig/petra>). Their distribution in the space of principal components is also shown in Fig. 1 (black dots). Most of these observations of Trojan asteroids have values of  $PC_1 \gtrsim 0$  compatible with featureless spectra, and values of  $PC_2 \gtrsim 0$  indicating that they have moderate to high spectral slopes. There are, however, some observations (circled dots in Fig. 1) that either depart significantly from the overall distribution of other Trojan observations, or they clearly fall within the region of featured spectra occupied by the S-type asteroids ( $PC_1 \lesssim 0.05$  and  $PC_2 \lesssim 0.2$ ). Direct inspection of the reflectance fluxes indicates that these observations are not compatible with featureless spectra or they show anomalous fluctuations, therefore we discarded them as well. The final sample contains 349 observations corresponding to 250 unique known

Trojan asteroids. Hereafter we will refer to this sample as the *Sloan sample*. The Sloan sample includes 200 observations of asteroids in the L4 swarm and 149 observations of the L5 swarm. About 40% of these observations correspond to asteroid family members.

It is worth mentioning that the main goal of our selection method is that it provides a sample of good quality observations from the SDSS-MOC3 that can be easily linked to family and to background (i.e. non family) asteroids. Our approach is different from that introduced by Szabó et al. 2007, who applied a kinematic criterion to select *candidate* Trojan asteroids within the SDSS-MOC3. These authors got a much larger sample of 1,187 observations, but these observations cannot be separated in those corresponding to family and to non family asteroids.

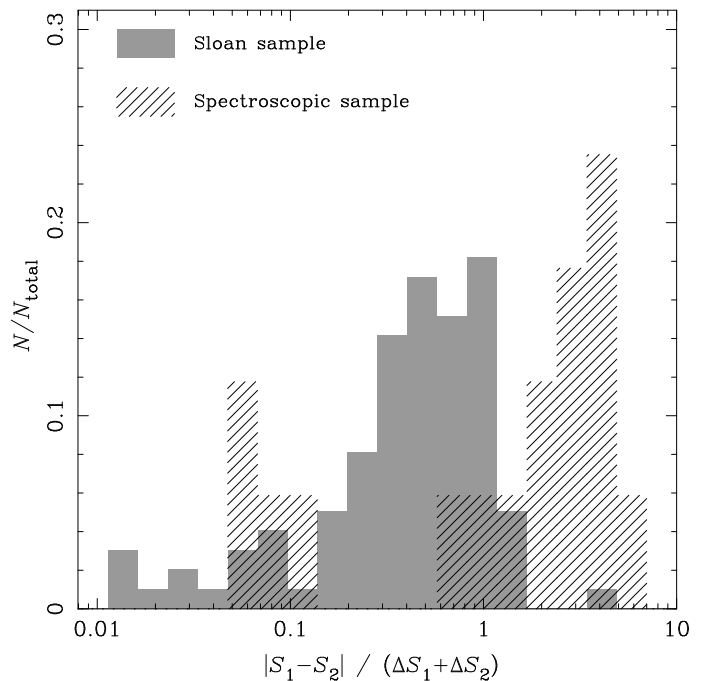
Each observation in our Sloan sample has been characterized by its equivalent spectral slope  $S$ , in  $\text{\AA}^{-1}$ . The slope was computed from a least-squares fit to a straight line passing through the fluxes  $F_g, F_r, F_i$  and  $F_z$ . This fit takes into account the individual errors of the fluxes to estimate the slope and its error  $\Delta S$ . Hereafter, we will refer to this set of 349 slopes as the *Sloan slopes*. Note that the flux  $F_u$  has not been used to compute the spectral slope. The reason for this is twofold: (i) we know, from spectroscopic observations, that the reflectance flux in the  $u$  band usually drops off and significantly deviates from the linear trend of the spectrum; (ii) we intend to compare the Sloan sample to a sample of spectroscopic data, described below, where most spectra do not cover the wavelengths  $\lesssim 5000 \text{\AA}$ . Since  $F_u$  does not contribute effectively to determine the slope, there is no harm in keeping its error unconstrained as we did.

Table 1 provides the list of all the known Trojan asteroids contained in our Sloan sample. This table also gives the estimated spectral slope,  $S$ , with its corresponding error,  $\Delta S$ , and the number of observations,  $N_{\text{obs}}$ , in the sample. For  $N_{\text{obs}} \geq 2$ , the slope given in this table is the weighted mean of the individual Sloan slopes, with the weights defined as  $1/(\Delta S)^2$ .

## 2.2. The Spectroscopic sample

The second data set analyzed here is a collection of 91 spectra corresponding to 74 individual Trojan asteroids published in the literature. All the spectra are defined in the visible wavelength range and have been obtained by different observational surveys, in particular: 3 spectra come from the SMASS1 survey (Xu et al. 1995), 2 spectra from the SMASS2 survey (Bus & Binzel 2002), 33 spectra from Bendjoya et al. (2004), 25 spectra from Fornasier et al. (2004), 13 spectra from the S3OS2 survey (Lazzaro et al. 2004), and 15 spectra from Dotto et al. (2006). Hereafter we will refer to this data set as the *Spectroscopic sample*. This sample includes 52 spectra of asteroids in the L4 swarm and 39 spectra of the L5 swarm. About 40% of these spectra correspond to asteroid family members.

To determine the spectral slope, each spectrum in the sample was first rebinned by applying a  $20 \text{\AA}$  running box average. The rebinned spectrum was then normalized to 1 at  $6230 \text{\AA}$  to make it comparable to the Sloan fluxes. Finally, the slope of the normalized spectrum was computed from a least-squares fit to a straight line in the interval  $5000\text{--}9200 \text{\AA}$ . This wavelength interval is similar to the one adopted to compute the Sloan slopes, and it is well covered by most spectra in our sample except for a few cases for which the fit had to be done over a smaller available range. Following the same approach as Fornasier et al. (2007), the error in the slope was estimated by adding an “ad-hoc” error of  $\pm 5 \times 10^{-6} \text{\AA}^{-1}$  to the standard error of the fit. The idea is



**Figure 2.** Distribution of the parameter  $\epsilon$  (see text) for the Sloan sample (gray histogram) and for the Spectroscopic sample (hatched histogram). Each histogram has been normalized such that its area is 1.

to account for uncertainties in the sample related to use of data obtained by different surveys. It is worth noting that the slopes computed here are not compatible with other published slopes (e.g. Jewitt & Luu 1990, Fornasier et al. 2007) due to different normalization wavelengths—usually  $5500 \text{\AA}$ —and also due to different wavelength intervals used to fit the data. In fact, our slopes may be up to 20% smaller than those published in the literature. Hereafter, we will refer to our set of 91 slopes as the *Spectroscopic slopes*, to distinguish them from the Sloan slopes.

Table 2 provides the list of all the known Trojan asteroids contained in our Spectroscopic sample. For asteroids with  $N_{\text{obs}} \geq 2$ , the slope shown in this table has been computed as the weighted mean of the individual Spectroscopic slopes. It is worth recalling that in Table 1 an asteroid with  $N_{\text{obs}} \geq 2$  had all its observations made by the same survey, i.e. the SDSS, while in Table 2 an asteroid with  $N_{\text{obs}} \geq 2$  had its observations made by different spectroscopic surveys.

## 2.3. Accuracy of the samples

The Sloan sample is  $\sim 4$  times larger than the Spectroscopic sample, which in terms of statistics does not appear to be a significant improvement. However, the Sloan sample is expected to be more homogeneous than the Spectroscopic sample because, in the former case, the observations come from the same survey, while in the latter they came from different surveys. Moreover, the spectroscopic surveys have been usually dedicated either to observe family members only (e.g. Fornasier et al. 2004, Dotto et al. 2006, Fornasier et al. 2007) or to observe background asteroids only (e.g. Lazzaro et al. 2004, Bendjoya et al. 2004). But the Sloan sample includes both family members and background asteroids observed by the same survey. The Sloan sample is also expected to include a significant amount of very small Trojans that spectroscopic surveys normally do not ob-

serve. Although the SDSS photometry is not as precise as spectroscopy, this is not crucial in the case of the Trojan asteroids because they all show featureless spectra that are properly characterized by the average spectral slope.

In order to verify the reliability of the Sloan and the Spectroscopic samples, we performed the following test. For each asteroid with  $N_{\text{obs}} \geq 2$  in Table 1 we computed the parameter

$$\epsilon = \frac{|S_1 - S_2|}{\Delta S_1 + \Delta S_2}$$

where  $S_i$  are the spectral slopes of two different observations of that asteroid. A value of  $\epsilon < 1$  indicates that this two observations are self-consistent, since their differences are within the individual errors. We can apply the same procedure to each asteroid with  $N_{\text{obs}} \geq 2$  in Table 2, and compare the results. In Fig. 2, we show the distribution of  $\epsilon$  values for the Sloan and Spectroscopic samples. The Sloan sample shows a good self-consistency among the observations of each asteroid with  $N_{\text{obs}} \geq 2$ . Since in most cases the individual errors are  $\sim 10\%$ , this result supports the idea of a quite homogeneous sample.

On the other hand, a significant fraction of the Spectroscopic sample shows differences among the observations of each asteroid with  $N_{\text{obs}} \geq 2$  that are beyond their errors. This may be explained by different observational conditions, different instrumental setup and different reduction processes among the different surveys. The inconsistency could be minimized by increasing the “ad-hoc” error introduced to estimate the slope error, but this “ad-hoc” error is already of  $\sim 10\%$ . Therefore, the result shown in Fig. 2 supports the idea that the Spectroscopic sample is less homogeneous than the Sloan sample, as expected.

### 3. Global distribution of spectral slopes

In this section we analyze the distribution of spectral slopes of the whole population of known Trojan asteroids included in our data samples, with particular attention to the asteroid families. First, we compare the Sloan and the Spectroscopic samples, and then we discuss each sample separately.

#### 3.1. Comparisons between the samples

In Fig. 3 we show the distribution of Sloan slopes (349 observations) compared to the distribution of Spectroscopic slopes (91 observations). Both distributions show a clear bimodality, that is more evident in the Sloan sample. This bimodality is related to the presence of two different taxonomic types among the Jupiter Trojans: (i) the D-type, with spectral slopes  $S \gtrsim 7.5 \times 10^{-5} \text{ \AA}^{-1}$ , that correspond to redder surfaces, and (ii) the P-type, with slopes  $1.5 \lesssim S \lesssim 7.5 \times 10^{-5} \text{ \AA}^{-1}$ , that correspond to less reddish colors. There is also a small amount of observations compatible with the C-type taxonomy, with slopes  $S \lesssim 1.5 \times 10^{-5} \text{ \AA}^{-1}$ , that correspond to more neutral colors. The limiting slopes between the taxonomic classes are estimated within a  $\pm 0.7 \times 10^{-5} \text{ \AA}^{-1}$  interval of tolerance, which is the approximate bin size in Fig. 3. It is worth stressing that these limiting slopes are *totally arbitrary*. Moreover, they are not compatible with the values adopted by the usual taxonomies, where the separation between the P- and D-types occurs at  $S \sim 5.5 \times 10^{-5} \text{ \AA}^{-1}$ . Nevertheless, our choice is based on the natural separation of the slopes induced by the bimodality in their distribution and it is valid as far as no mineralogical constraint is known to define the P and D taxonomic types.

The D-type observations dominate over the P-type in the approximate proportion  $\frac{2}{3} : \frac{1}{3}$ , but the Sloan sample shows a larger abundance of P-type relative to D-type than the Spectroscopic sample. The bimodality observed in Fig. 3a has also been reported by Szabó et al. (2007) analyzing SDSS-MOC3 colors<sup>1</sup>. The Sloan slopes appear more tightly clustered than the Spectroscopic slopes, which might be related to the less homogeneity of the Spectroscopic sample. Nevertheless, the Sloan slopes appear well correlated to the Spectroscopic slopes, as shown in Fig. 3b for the few observations corresponding to asteroids included in both samples.

To analyze the distribution of spectral slopes of the asteroid families, we first proceeded to identify the different families in each Trojan swarm. We used the catalog of 1702 Trojan asteroids with known resonant proper elements maintained by the PETrA Project (Beaugé & Roig 2001) and applied to this catalog the Hierarchical Clustering Method (HCM, Zappalà et al. (1995)). The mutual distance between any pair of asteroids in the proper elements space was computed according to the metric

$$d = \left[ \frac{1}{4} \left( \frac{\delta a}{a_0} \right)^2 + 2(\delta e)^2 + 2(\delta \sin I)^2 \right]^{1/2}$$

(Milani 1993), where  $\delta a$ ,  $\delta e$  and  $\delta \sin I$  are the differences in proper semi-major axis, proper eccentricity and proper sinus of inclination, respectively, between the given pair of asteroids, and  $a_0 = 5.2026 \text{ AU}$  is the average proper semi-major axis of the Trojan population. Those bodies for which  $d \leq d_{\text{cut}}$  were clustered together to form the families. The cutoff value  $d_{\text{cut}}$  was chosen to be  $110 \text{ m s}^{-1}$  for the L4 swarm and  $120 \text{ m s}^{-1}$  for the L5 swarm, which are comparable to the corresponding quasi-random level of each swarm<sup>2</sup>. We have verified that values of  $d_{\text{cut}}$  within  $\pm 10 \text{ m s}^{-1}$  around the above values produce practically the same results. Clusters with less than 8 members in the L4 swarm and with less than 6 members in the L5 swarm were considered statistical fluctuations and were disregarded. For a detailed explanation on the definition of  $d_{\text{cut}}$  and the application of the HCM to the Trojan case refer to Beaugé & Roig (2001). The distribution of the detected families in the space of proper eccentricity and inclination is shown in Fig. 4.

In Fig. 5, we show the slope distribution of family members (panel a) compared to the background asteroids (panel b). The gray histograms correspond to the Sloan sample, while the hatched histograms correspond to the Spectroscopic sample. Except for a few background asteroids with very small and even negative slopes (these latter observed by Bendjoya et al. (2004)), the distribution of Sloan slopes of background asteroids is comparable to the distribution of Spectroscopic slopes, both showing a clear abundance of D-type asteroids. The situation is quite different for the family members, since the Sloan sample shows a clear bimodality that is not observed in the Spectroscopic sample. It is worth noting that the Sloan sample contains about 3 times more observations of family members and goes much deeper in absolute magnitude than the Spectroscopic sample. This result may indicate that family members contribute with a significant amount of the P-type asteroids found among the Trojan swarms. It also indicates that families appear to be bluer than the background.

<sup>1</sup> Indeed, the principal color  $t_c^*$  introduced by these authors is strongly correlated to both the second principal component  $PC_2$  and the spectral slope  $S$ .

<sup>2</sup> The quasi-random level is the maximum level of statistical significance of the HCM.

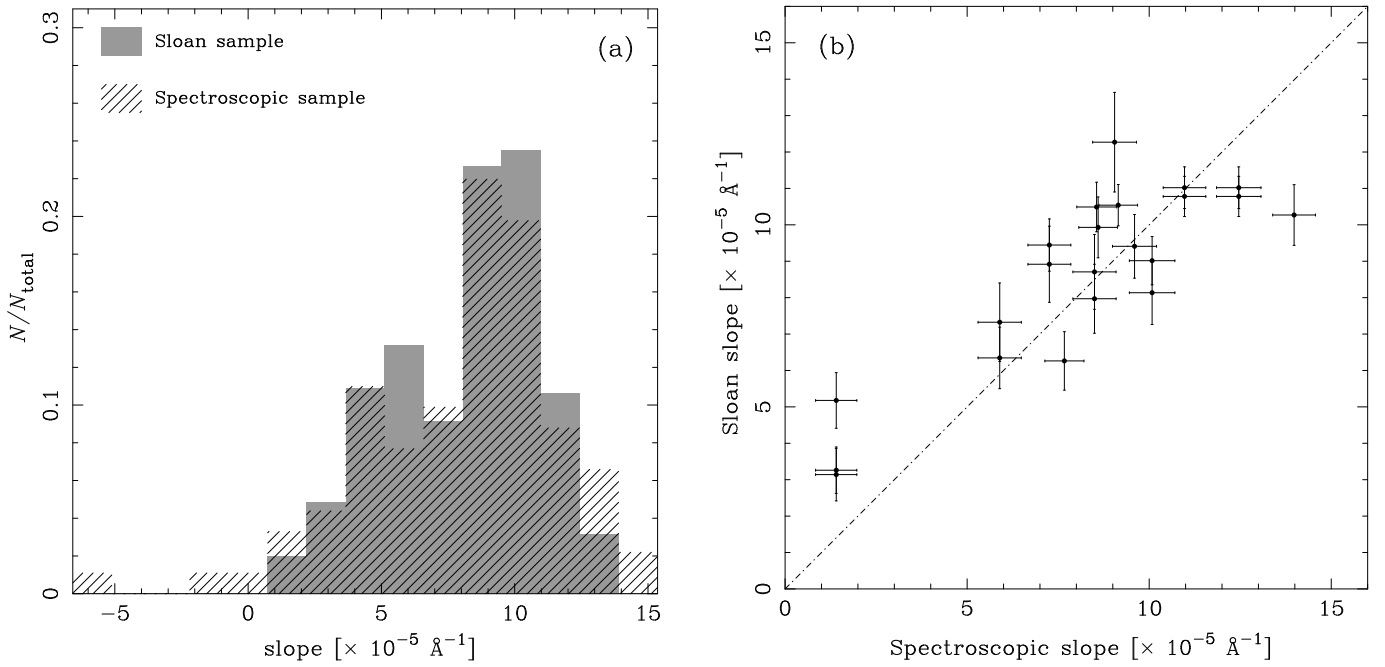


**Figure 3.** (a) Distribution of spectral slopes from the Sloan sample (349 observations, gray histogram) and from the Spectroscopic sample (91 observations, hatched histogram). Each histogram has been normalized such that its area is 1. Both distributions show a bimodality related to the presence of two taxonomic types: P-type (smaller slopes) and D-type (larger slopes). (b) Comparison between the Spectroscopic slopes and the Sloan slopes from observations of asteroids included in both samples

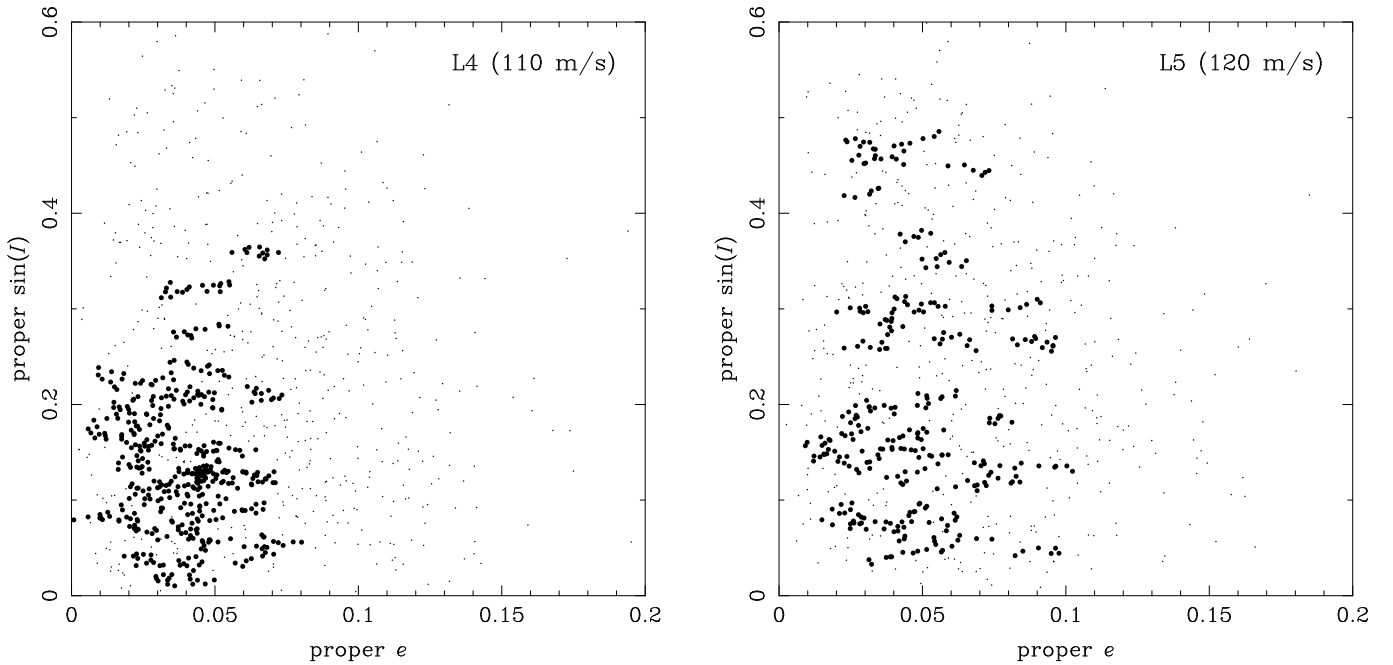


**Figure 4.** *Left panel.* Asteroid families (big dots) identified in the L4 swarm, projected in the space of proper eccentricity and inclination. Background asteroids are represented by small dots. The cutoff level is  $110 \text{ m s}^{-1}$ . *Right panel.* The same but for the L5 swarm. The cutoff level is  $120 \text{ m s}^{-1}$ .

### 3.2. Global analysis of the Sloan sample

It is well known that asteroid families do not appear equally distributed among the L4 and L5 swarms. While the families in L4 are more conspicuous and tend to form large clusters, the families in L5 are smaller and tighter. The total number of families is also larger in L4 than in L5. Thus, it is interesting to analyze the distribution of Sloan slopes separately in each swarm. Figure 6a

shows the distribution of Sloan slopes of family members in the L4 swarm (gray histogram) and in the L5 swarm (outlined histogram). The difference between the swarms is notorious. While in L4 the Sloan slopes show a predominance of P-type asteroids among the families, the L5 families appear dominated by D-type asteroids. The families in L5 are significantly redder than those in L4. On the other hand, the slope distribution of background as-

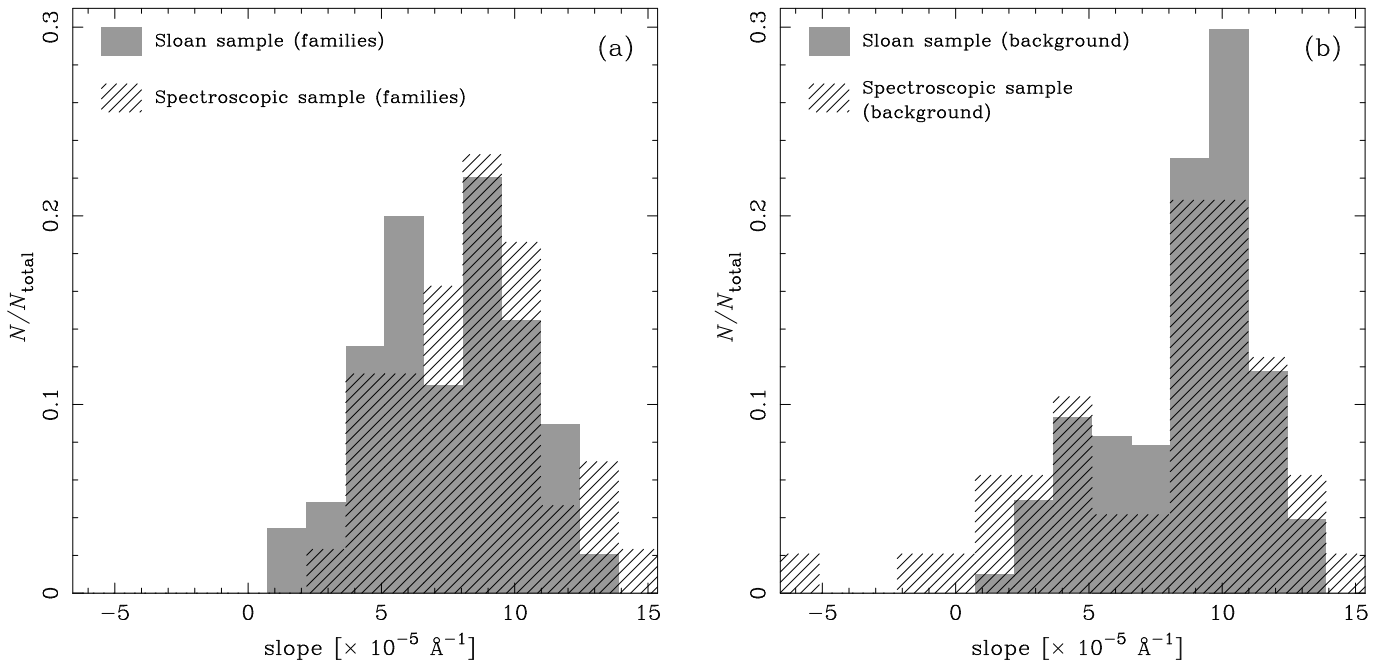


**Figure 5.** (a) Distribution of spectral slopes of observations corresponding to family members. The gray histogram correspond to the Sloan slopes and the hatched histogram to the Spectroscopic slopes. (b) The same but for the observations corresponding to background asteroids. Each histogram has been normalized such that its area is 1.

teroids, shown in Fig. 6b, is almost the same in the two swarms, with a significant peak of D-type asteroids.

The behavior observed in Fig. 6a,b may explain the different color distributions between the L4 and L5 swarms reported by Szabó et al. (2007) from the analysis of SDSS-MOC3 colors. These authors pointed out that the amount of redder asteroids (higher slopes), relative to the bluer ones (smaller slopes), is much larger in the L5 swarm than in the L4 swarm. The situation is clearly illustrated in Fig. 6c. They explained this difference on the basis of an observational selection effect that causes to detect more asteroids with high orbital inclination, relative to those with low orbital inclination, in the L5 swarm compared to the L4 swarm. Since there is a clear correlation between color and orbital inclination, such that the bluer bodies have low inclinations while the redder ones are predominantly found at high inclinations, and since this correlation appears to be the same in both swarms, Szabó et al. (2007) conclude that it is natural to find a large fraction of redder bodies in the L5 swarm. The authors tried to overcome the observational selection effect by separating their observations in those corresponding to high inclination asteroids ( $> 10^\circ$ ) and those corresponding to low inclination bodies ( $< 10^\circ$ ), and showing that, with this separation, the differences between L4 and L5 almost disappear.

We believe, however, that a separation in terms of asteroid families and background asteroids, instead of orbital inclinations, provides a much better explanation, since it is clear from Fig. 6 that the swarms differ in their color distributions due to the presence of the asteroid families. The advantage of this scenario is that it has a physical basis and does not require to invoke any strange observational bias. It is also interesting to analyze the color-inclination correlation in terms of asteroid families. In Fig. 7 we show the distribution of asteroid family members (panel a) and background asteroids (panel b) in the plane of spectral slope vs. orbital inclination. Dots and crosses represent the L4 and L5 observations, respectively. The family members do not show any apparent correlation between color and inclination, contrary to

the background that it is strongly correlated. This correlation appears to be the same in both swarms, as Szabó et al. (2007) conjectured.

We must note that the separation in low and high inclination populations proposed by Szabó et al. (2007) partially works to explain the different color distributions between L4 and L5 because the family members are not uniformly distributed in terms of proper inclination. In fact, the families in the L4 swarm are mostly concentrated at low inclinations while the families in L5 spread over a wider range of proper inclinations, as we can see in Fig. 4. If we consider only the high inclination asteroids ( $\sin I \gtrsim 0.2$ ), then the L4 swarm is dominated by background asteroids (Fig. 4) which are predominantly red (Fig. 7b). The L5 swarm has a larger proportion of asteroid families at high inclinations (Fig. 4), but these are also predominantly red (Fig. 6a) as the background. Thus, both swarms show the same color distribution at large inclinations. On the other hand, if we consider the low inclination asteroids ( $\sin I \lesssim 0.2$ ), the asteroid families significantly contribute to the slope distribution. While the background tends to be bluer (Fig. 7b), the families cover a wider range of colors (Fig. 6a) and this tends to disguise the differences in slope distribution between the swarms. This is precisely the result found by Szabó et al. (2007).

Another interesting result concerns the correlation between spectral slope and absolute magnitude (or size). Figure 8 is analogous to Fig. 7, but in terms of absolute magnitude instead of orbital inclination. If we eliminate the few large bodies ( $H \lesssim 9$ ) from the sample then the families (Fig. 8a) do not show any apparent correlation, but the background asteroids (Fig. 8b) shows a weak correlation since bodies in the range  $9 \lesssim H \lesssim 11$  are predominantly red. Note that, if we consider together the families and the background, the slope-size correlation is disguised and this is probably the reason why Szabó et al. (2007) did not detect this correlation in their analysis.

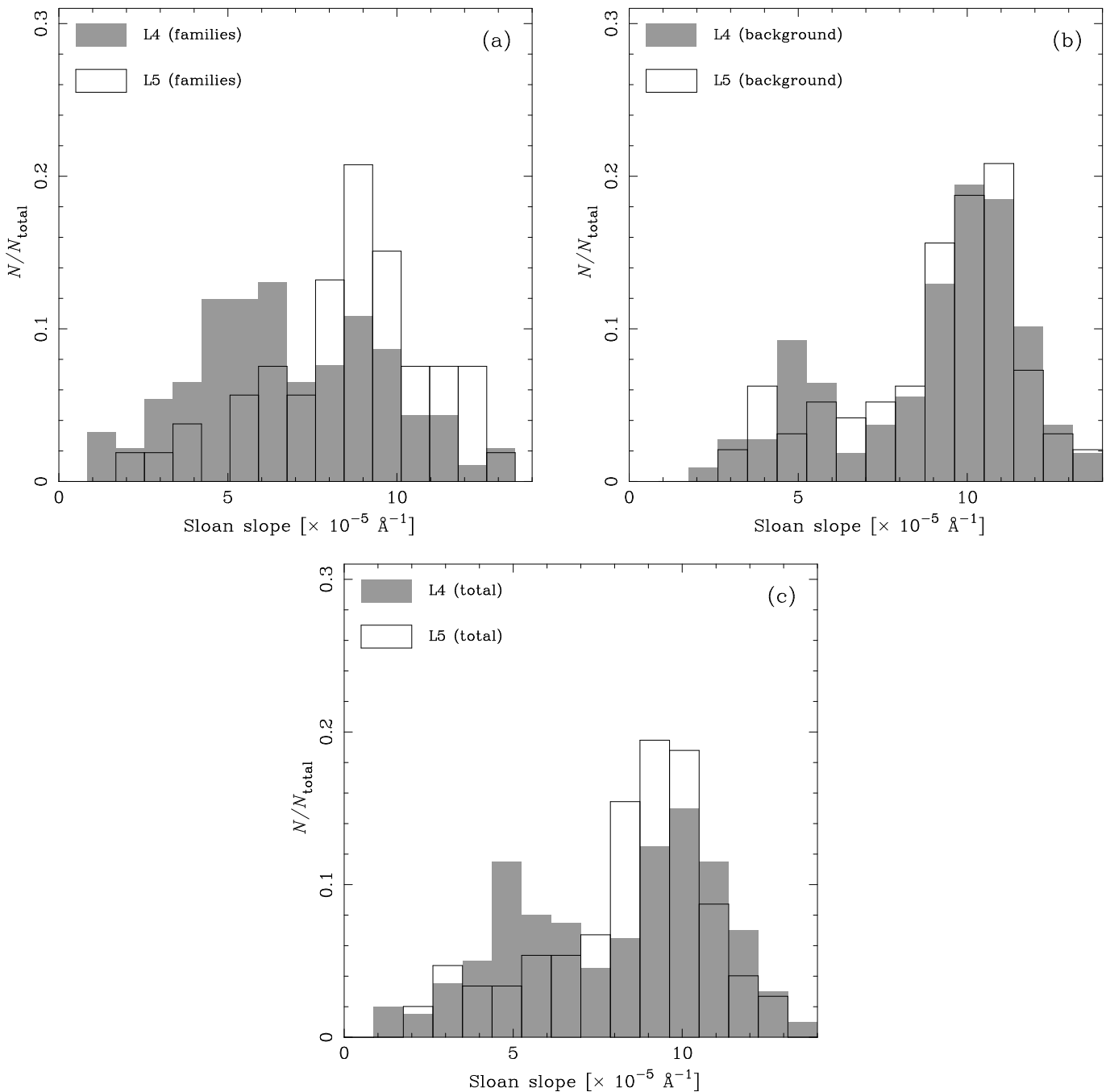


**Figure 6.** (a) Distribution of the Sloan slopes of family members only. The gray histogram correspond to the L4 swarm and the outlined histogram to the L5 swarm. (b) Same as (a) but for the background asteroids only. (c) Same as (a) but for both family members and background asteroids together. Each histogram has been normalized such that its area is 1.

The results of Figs. 7b and 8b led to conclude that large background asteroids in both Trojan swarms tend to be redder and tend to be located at large orbital inclinations.

### 3.3. Global analysis of the Spectroscopic sample

The behavior observed in Fig. 6 is not reproduced among the Spectroscopic sample. This is probably due to the fact that our Spectroscopic sample is deficient in observations of family members in the L4 swarm. In fact, the actual population in the L4 swarm is at least  $\sim 1.6$  times larger than in the L5 swarm,

but our Spectroscopic sample includes about the same amount of family members in both swarms.

Besides, neither the correlation between slope and inclination, nor the one between slope and size are observed in the Spectroscopic sample. This may be due to the smaller number of objects contained in the sample and to its less homogeneity. It is interesting to note that the background of the Spectroscopic sample includes some large P-type asteroids and also some high-inclination P-type asteroids that are not observed in the Sloan sample.

An analysis of a much larger data set of spectroscopic data has been performed by Fornasier et al. (2007). Their sam-

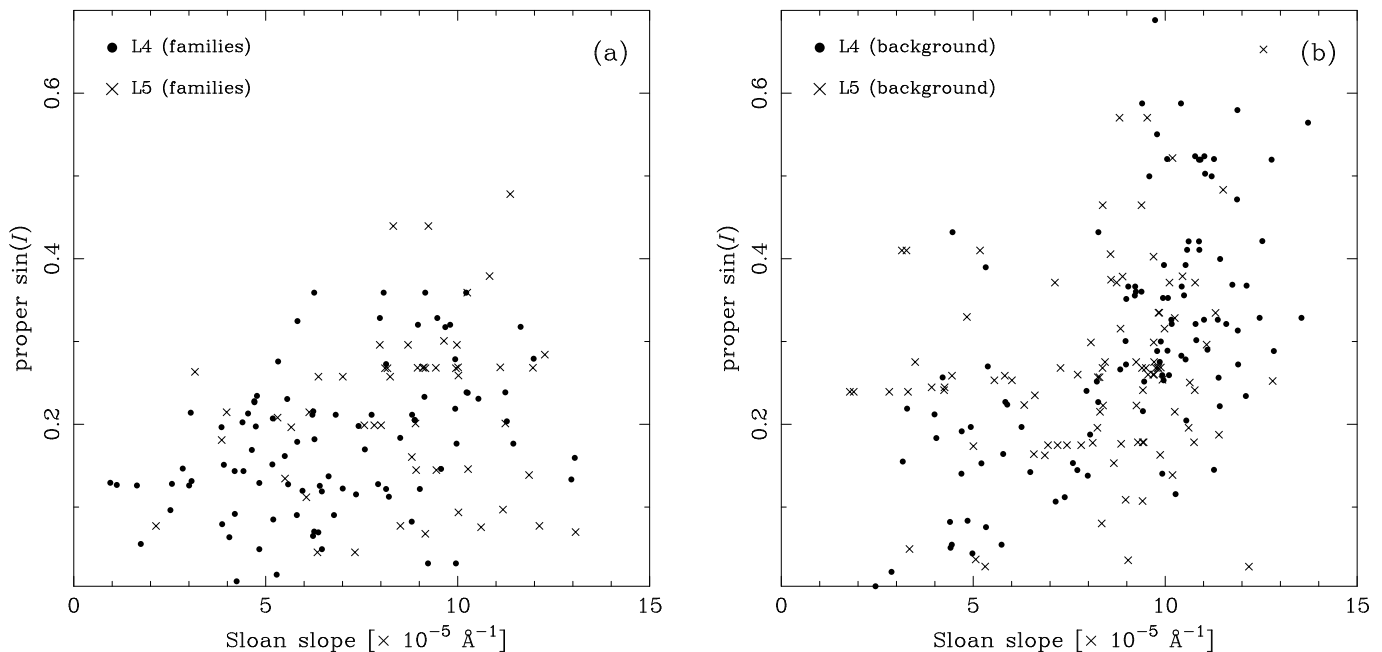


**Figure 7.** (a) Distribution of the Sloan slopes of family members as a function of proper inclination. Dots correspond to the L4 swarm and crosses to the L5 swarm. (b) Same as (a) but for the background asteroids. Note the significant lack of high-inclination background asteroids with small slopes (P-types).

ple includes the same observations that we include in our Spectroscopic sample plus other spectroscopic observations from Jewitt & Luu (1990), Fitzsimmons et al. (1994) and from themselves, totaling 142 different Trojan asteroids. They found a situation very similar to the one observed in Fig. 6c, indicating that the L4 swarm has a larger fraction of P-type asteroids, relative to D-type, compared to the L5 swarm. Fornasier et al. (2007) did not find any slope-size correlation, although they detected that the distribution of spectral slopes is narrower at large sizes. In fact, from figure 9 of their paper, it is possible to infer a slight predominance of D-type asteroids among the large asteroids ( $50 \lesssim D \lesssim 120$  km). This situation would be similar to the one obtained in the range ( $9 \lesssim H \lesssim 11$ ) by overlapping the two panels in Fig. 8. An analysis of the slope-size relation using the data in Fornasier et al. (2007) and separating asteroid families from background asteroids might help to check whether the result shown in Fig. 8 correspond to a real correlation or is just an artifact of our Sloan sample.

### 3.4. Discussion

The fact that only the background asteroid show correlations between spectral slope, absolute magnitude and orbital inclination, and that the correlations are similar in both the L4 and L5 swarms, may put important constraints to the origin and evolution of Jupiter Trojans. No dynamical mechanism among the Trojans is known to favor the evolution of asteroids according to their size or to their surface physical properties<sup>3</sup>. Therefore, these correlations may have a primordial origin. Alternatively, the correlations may be the by-product of collisional evolution. We speculate here about two possible scenarios.

One scenario involves the idea that the P and D classes are related to different mineralogies and, consequently, to different material strengths. Let us assume that P-type asteroids are eas-

ier to breakup than D-type asteroids. Recall that this is just an assumption and there is no evidence, neither observational nor theoretical, to support it. Therefore, large P-type asteroids will tend to fragment in smaller bodies while large D-type asteroids will tend to remain intact, causing a loss of large P-type asteroids as suggested in Fig. 8b. In addition, fragments from P-type asteroids may acquire larger ejection velocities after a breakup than fragments from D-type asteroids. Since the islands of stability around L4 and L5 shrink at large inclinations (e.g. Marzari et al. 2003, Schwarz et al. 2004), many of these P-type fragments might be ejected beyond the stability limits of the swarms causing the lack of high-inclination P-type asteroids observed in Fig. 7b. The predominance of P-type asteroids among the L4 families is in line with this scenario but, on the other hand, the predominance of D-type asteroids among the L5 families is against it.

Another scenario involves the idea that the P and D classes represent the same mineralogy but modified by some aging process, like the space weathering. Let us assume that the space weathering produces a reddening of the surfaces, so D-type asteroids have older surfaces than P-type asteroids. The surfaces may be renewed either by disruptive collisions, that expose the “fresh” interior of the parent body, or by resurfacing collisions. We could expect that both collisional phenomena are more frequent at low inclinations than at high inclinations, and more frequent among the small bodies than among the large ones. Thus, high inclination and large asteroids would be, on average, older (i.e. redder) than low inclination and small ones, in agreement with Figs. 7b and 8b. This scenario would also imply that families in L5 are, on average, older than those in L4.

The above scenarios have several limitations because none of them are well constrained. The mineralogy associated to the P- and D-types is totally unknown. In fact, some authors claim that D-type asteroids would be more fragile than P-types (Dahlgren et al. 1997). The actual effect of space weathering on spectrally featureless surfaces and the time scale to produce a

<sup>3</sup> The Yarkovsky effect, that depends on size and surface properties, also depends on the Sun distance and it is negligible at 5 AU.



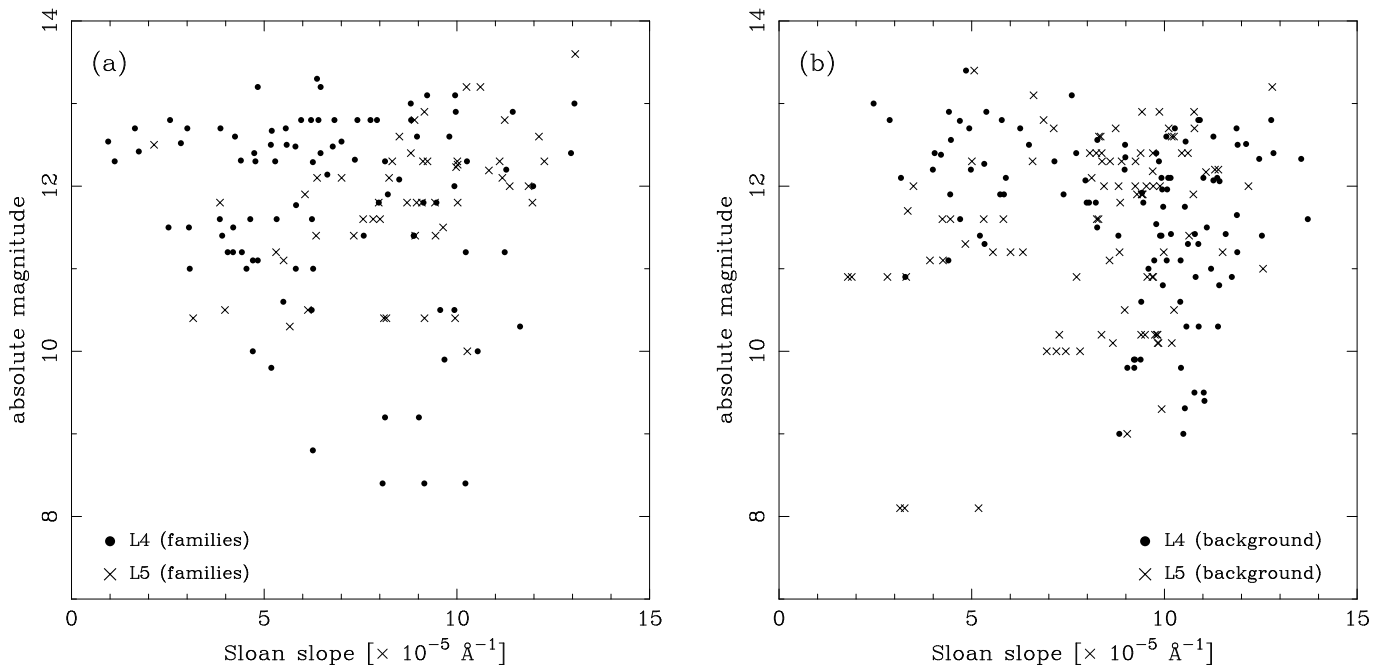


**Figure 8.** (a) Distribution of Sloan slopes of family members as a function of absolute magnitude. Dots correspond to the L4 swarm and crosses to the L5 swarm. (b) Same as (a) but for the background asteroids. Note the significant lack of large background asteroids with small slopes (P-types).

significant change in the spectral slope are also unknown. Some authors propose that the space weathering would tend to neutralize the colors of initially red surfaces (Moroz et al. 2004), so P-type asteroids would have older surfaces than D-types<sup>4</sup>. The rate of collisional events that can produce disruption or resurfacing depending on diameter and orbital inclination is poorly constrained. Last, but not least, it may happen that what we observe is the product a complex combination of all these effects.

#### 4. Distribution of spectral slopes for selected asteroid families

In the previous section we discussed the global distribution of spectral slopes among Trojan asteroid families and background asteroids. In this section we analyze some particular families, selected in view of their interest and the number of its members contained in both the Sloan and the Spectroscopic samples. For this analysis we did not consider all the observations available in the samples. Instead, we used the slopes listed in Tables 1 and 2 (i.e. for asteroids with more than one observation we consider the average slope of the observations).

<sup>4</sup> An interesting idea is that the space weathering may have two phases: an initial phase in which it produces a reddening of the surfaces up to a saturation level, and a second phase in which it produces the opposite effect, leading to more neutral color surfaces, together with a reduction of the overall albedo. Within this scenario, P-type asteroids could have either too young (high albedo) or too old (low albedo) surfaces, while D-types would have mid-age surfaces. D-type asteroids would also be, on average, more numerous because an asteroid would spend most of its life showing a reddish surface, unless a collision modifies it. This might be causing the overall abundance of D-type asteroids among the Trojans. The knowledge of the albedo values for a large amount of Jupiter Trojans might help to better constrain this scenario. Unfortunately, up to now very few Trojans have known albedos

#### 4.1. Families in the L4 swarm

##### 4.1.1. The Menelaus clan

Several families in the L4 swarm merge together at high values of the cutoff ( $d_{\text{cut}} > 125 \text{ m s}^{-1}$ ) to form a big clan of families, similar to the Flora clan in the inner asteroid Main Belt. This clan gets its name after the main member, asteroid (1647) Menelaus. The structure of the Menelaus clan is shown in Fig. 9 (left) in the form of a dendrogram (Zappalà et al. 1995). Each stalactite in the dendrogram represents a different family within the clan, and it is easy to see how the families are better resolved as we go to lower values of the cutoff. The word “clan” invokes some kind of common origin, but the fact that several families form a clan does not necessarily imply that they all come from the same ancestor. The taxonomic analysis of the clan members may help to better understand this problem.

As seen in Fig. 9, the more robust family of the clan is the Menelaus family itself, which counts more than 100 members at the quasi random level ( $\sim 104 \text{ m s}^{-1}$ ) and represents the largest family in the L4 swarm. The small families of Telamon, Melanthios and Podarkes separate from the Menelaus family at lower cutoffs but they soon disappear. On the other hand, the Eurybates family appears as a very robust cluster that survives down to very small cutoffs. Indeed, the Eurybates family forms a very tight cluster within the Menelaus family, as shown in Fig. 9 (right). From the solely analysis of Fig. 9 it is difficult to decide whether the Eurybates family is a sub-cluster of the Menelaus family, i.e. a family formed by the secondary breakup of a former Menelaus family member, or the Eurybates and Menelaus families are two different families that simply overlap in the space of proper elements.

The taxonomy of these two families has been analyzed by Dotto et al. (2006 - hereafter D06) and by Fornasier et al. (2007 - hereafter F07), who obtained spectra of 3 members of the Menelaus family and 17 members of the Eurybates family. These authors found that the Menelaus family is mostly a D-type fam-

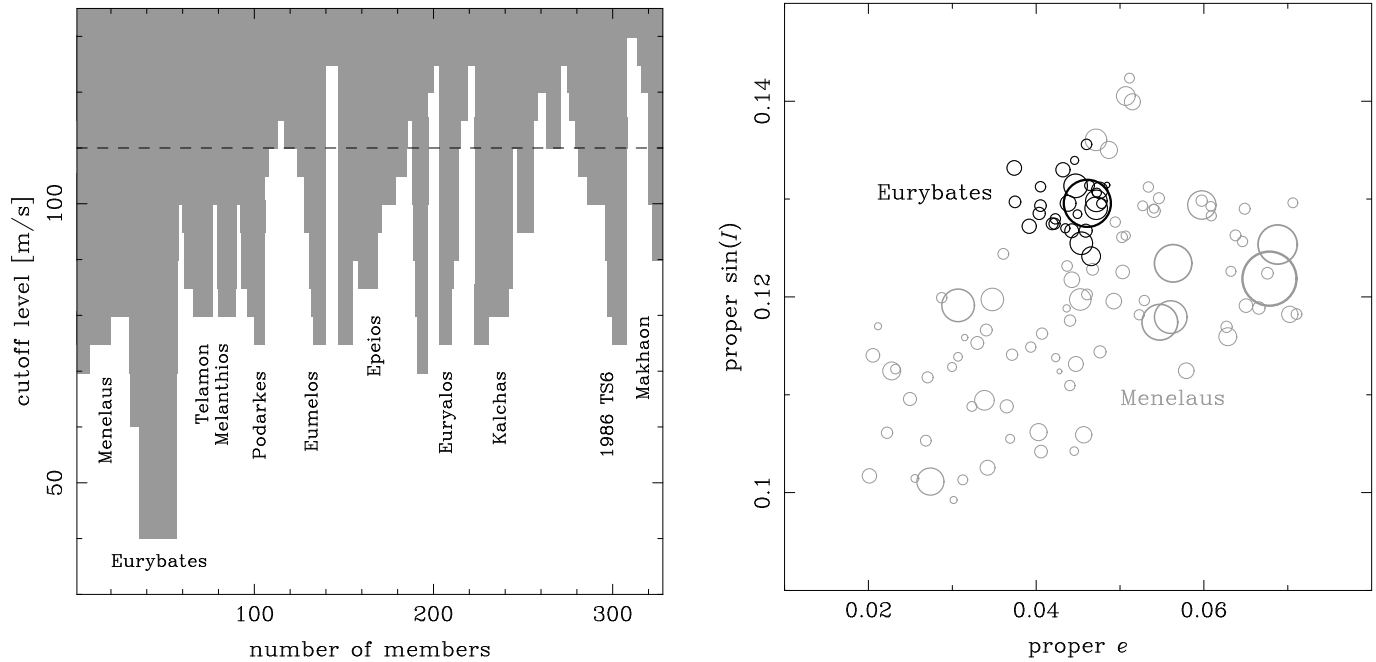


**Figure 9.** *Left panel.* Dendrogram of the Menelaus clan, indicating the main families identified. The dashed horizontal line is the cutoff used in this study. *Right panel.* Distribution in the space of proper elements of the Menelaus family (gray circles) as detected at  $d_{\text{cut}} = 110 \text{ m s}^{-1}$ , and of the Eurybates family (black circles) as detected at  $d_{\text{cut}} = 70 \text{ m s}^{-1}$ . The size of each circle is proportional to the asteroid size.

ily, but the Eurybates family is dominated by C-type asteroids. A slightly different result is obtained from the analysis of our data samples.

Figures 10a,b show the spectral slopes of the Menelaus and Eurybates families as a function of the absolute magnitude. At large sizes ( $H < 11$ , that correspond to  $\sim 40 \text{ km}$ ), the Menelaus family shows a slight predominance of D-type asteroids –(1749) Telamon, (5258) 1989 AU1 and (13362) 1998 UQ16– compared to one P-type asteroid –(5244) Amphilochos–, and another asteroid –(1647) Menelaus– that appears to be a P-type but could be classified as D-type if we account for its error and recall that the limiting slope of  $7.5 \times 10^{-5} \text{ \AA}^{-1}$  between the P- and D-types has a  $\pm 0.7 \times 10^{-5} \text{ \AA}^{-1}$  uncertainty (actually, D06 classified this asteroid as D-type). On the other hand, at the small sizes ( $H > 11$ ) the family is clearly dominated by P-type asteroids.

The results for the Eurybates family (Fig. 10b) are more in line with the findings of F07, although we do not detect a predominance of C-type asteroids due to the small amount of observations in the Sloan sample. Three asteroids –(9818) Eurymachos, (18060) 1999 XJ166 and (24426) 2000 CR12– are P-type and one asteroid –(43212) 2000 AL113– is C-type. These four asteroids got the same taxonomic classification by F07. There is also one asteroid –(65225) 2002 EK44– that appears to be a P-type but due to its error can be classified as C-type, in agreement with F07. The last body –2002 AE166– is a C-type asteroid and was not observed by F07.

Figures 10c,d show the spectral slopes of other members of the Menelaus clan: the Epeios and 1986 TS6 families. The Epeios family has not been previously observed by any spectroscopic survey, so the Sloan slopes shown here provide the first taxonomic information about this family, which appears constituted mostly by P-type asteroids, especially at the large sizes. On

the other hand, the 1986 TS6 family has been observed by D06<sup>5</sup> and F07. The available data, including the Sloan slopes, indicate that this family has two well separated components, one P-type and one D-type, regardless of bodies size. Note, however, that these two components cannot be resolved in terms of proper elements, i.e. the P- and D-type members are mixed in the same cluster even for the smallest possible cutoffs. The largest asteroid in the family, (5025) 1986 TS6, shows significantly different values of Sloan slope ( $5 \times 10^{-5} \text{ \AA}^{-1}$ ) and Spectroscopic slope ( $15 \times 10^{-5} \text{ \AA}^{-1}$ ), but the latter has been computed from a very noisy spectrum of Bendjoya et al. (2004) so its anomalous large value should be considered with care.

The above results points to the idea that not only the Menelaus clan as a whole, but also the individual families are quite heterogeneous in terms of taxonomic classes, including from the reddest D-type asteroids to the neutral-color C-type ones. Note also that the spectral slopes do not show any particular trend with size.

#### 4.1.2. Other families

Figure 11 shows the distributions of spectral slopes in terms of absolute magnitude of two families that are not members of the Menelaus clan: 1986 WD and Laertes. The 1986 WD family has been studied by D06 and F07 who found a wide range of slopes, from the D- to the C-type. The Sloan slopes tend to confirm these findings. This family is small ( $\sim 15$ -20 members) and at cutoff values slightly smaller than the quasi random level it loses half of its members. The family is no longer identified at cutoffs smaller than  $95 \text{ m s}^{-1}$ . Therefore, the diversity of taxo-

<sup>5</sup> These authors refer to it as the Makhaon family due to the large cutoff used, but it is clear from Fig. 9 that Makhaon is a different family. This has been correctly addressed by F07.

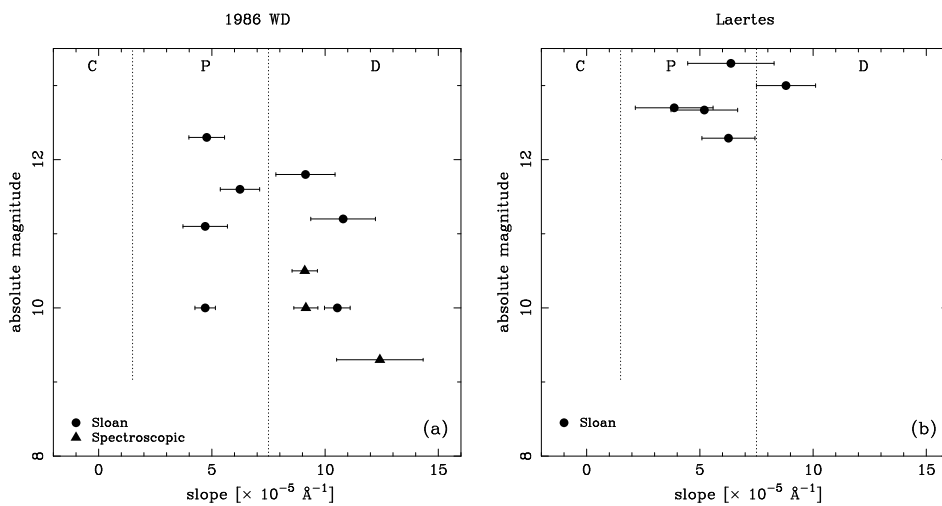
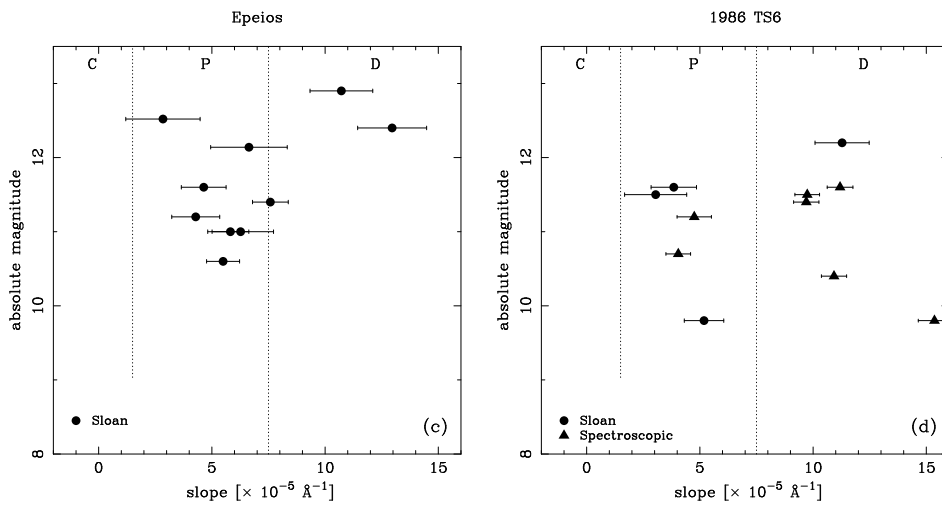
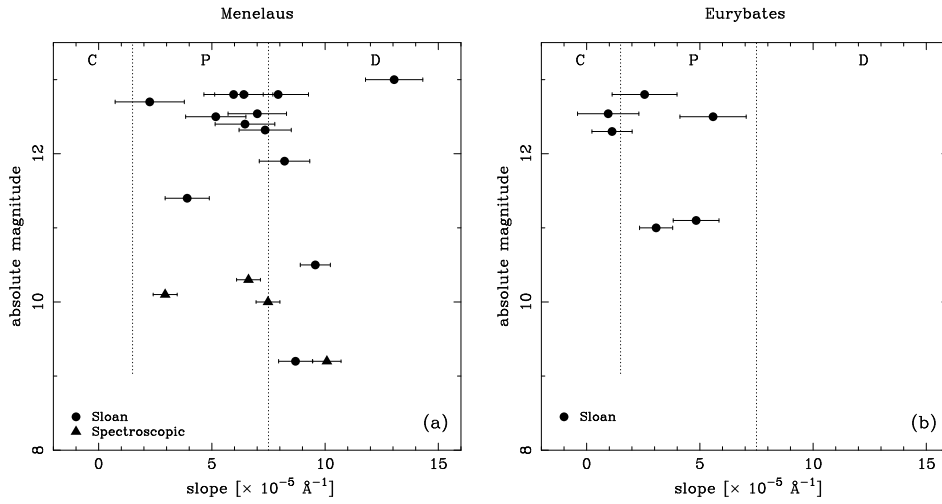


**Figure 10.** Distribution of Sloan slopes against absolute magnitude for four families of the Menelaus clan. Full circles correspond to Sloan slopes. Triangles correspond to Spectroscopic slopes. The vertical dotted lines define the slope transition, within  $\pm 0.7 \times 10^{-5} \text{ \AA}^{-1}$ , between the different taxonomic classes indicate above the plots.

nommic classes may be related to a significant contamination of interlopers.

The case of the Laertes family is somehow different. This family is also small ( $\sim 15$ -20 members) but it survives down to cutoff  $80 \text{ m s}^{-1}$  loosing only 40% of its members. All the members are small bodies ( $H > 11$ ), including (11252) Laertes. The few members contained in the Sloan sample (the family has never been observed spectroscopically) show a quite homogeneous distribution of spectral slopes, all belonging to the P-type.

Unfortunately, this family is located at a very small inclination ( $\sin I \sim 0.08$ ), and it cannot be distinguished from the background also dominated by P-type asteroids. The identification of the Laertes family as a real P-type family relies more in the accuracy of the HCM than in the distribution of its spectral slopes.

Other interesting cases are the high inclination families in the L4 swarm. There are only three of these families, with  $\sin I > 0.25$ : Hektor, Teucer and Sinon. The distribution of the respective spectral slopes are shown in Fig. 12. Hektor and Sinon

**Figure 11.** Same as Fig. 10 but for two families in the L4 swarm.

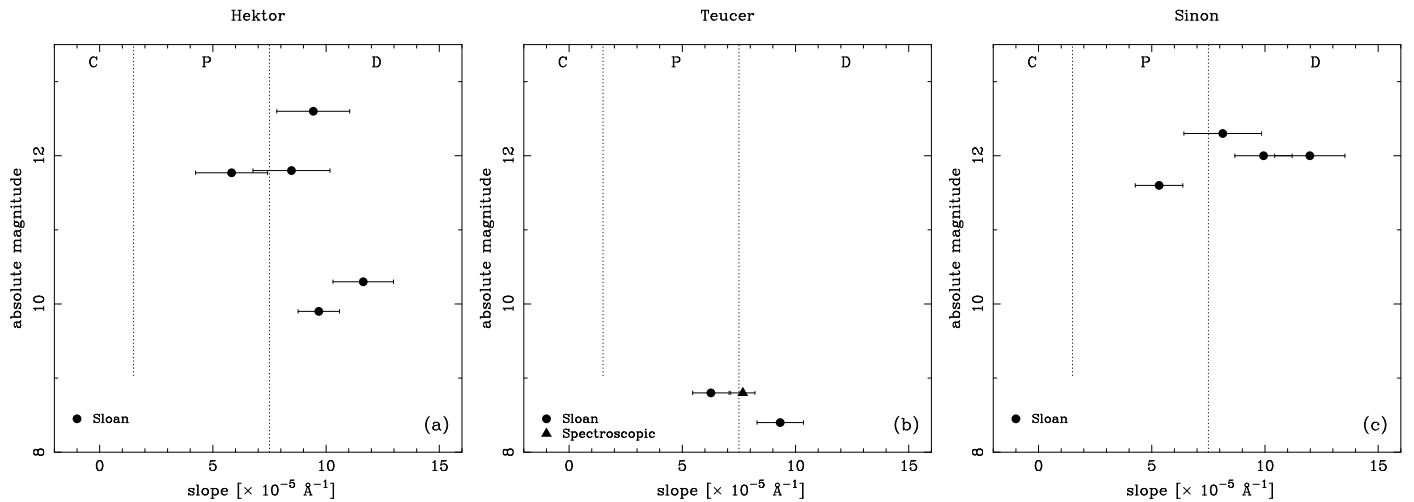


**Figure 12.** Same as Fig. 10 but for three high-inclination families in the L4 swarm.

families have not been observed by previous spectroscopic surveys, and the Sloan slopes provide the first clues about their taxonomic composition. The slopes in Fig. 12 point to a predominance of D-type asteroids, making these families indistinguishable from the background.

## 4.2. Families in the L5 swarm

### 4.2.1. The Anchises clan

The L5 swarm has its own clan of families, although it is somehow different from the Menelaus clan in L4. The Anchises clan, named after asteroid (1173) Anchises, is quite tight and constituted by only five families identified at  $d_{\text{cut}} = 120 \text{ m s}^{-1}$ : Panthoos, Polydoros, Sergestus, Agelaos and 1999 RV165. All these families merge in the clan at  $d_{\text{cut}} = 150 \text{ m s}^{-1}$ . The taxonomic analysis of this clan indicates that it is populated by both P- and D-type asteroids covering a wide range of spectral slopes. But at variance with the Menelaus clan, the individual families of the Anchises clan appear to be more homogeneous in terms of taxonomy.

The Panthoos family appear to be a P-type family (Fig. 14a) and it is well distinguishable from the background, dominated by D-type asteroids. This is a quite robust family that remains isolated over a wide range of cutoff values, from 90 to  $140 \text{ m s}^{-1}$ . Its distribution in the space of proper elements for  $d_{\text{cut}} = 130 \text{ m s}^{-1}$  is shown in Fig. 13. It is worth noting that F07 studied this family and found that it is a D-type family. However, due to an incorrect choice of the cutoff level, all the 8 asteroids that they used to perform their classification are not actual members of the Panthoos family but of the Sergestus family. These two families merge together at  $d_{\text{cut}} > 140 \text{ m s}^{-1}$ .

The Polydoros family is another example of a quite robust family that is detected down to cutoff  $90 \text{ m s}^{-1}$ . This family merges with the Sergestus family for  $d_{\text{cut}} \geq 130 \text{ m s}^{-1}$  to form the single Polydoros family shown in Fig. 13. The distribution of spectral slopes of the Polydoros (+Sergestus) family, shown in Fig. 14b, indicates that this is a quite homogeneous D-type family. Interestingly, the spectral slope of (4829) Sergestus measured by F07 indicates that this asteroid is likely to be a P-type, so it may be an interloper. Recall, however, that the Polydoros and Sergestus families are taxonomically indistinguishable from the background and this makes difficult the discussion about interlopers.

The Agelaos and 1999 RV165 families are somehow different from the other families of the Anchises clan. None of them survive down to small cutoffs and they appear less homogeneous in terms of taxonomy. Their distribution in proper elements is shown in Fig. 13. At  $d_{\text{cut}} > 135 \text{ m s}^{-1}$ , the Agelaos family incorporates asteroid (1173) Anchises and becomes the Anchises family. At the same cutoff, the 1999 RV165 family becomes the Antenor family after incorporating asteroid (2207) Antenor. These two families merge together at  $d_{\text{cut}} > 145 \text{ m s}^{-1}$ .

The 1999 RV165 family has only one member in the Sloan sample classified as P-type, so we cannot say too much about it. The Agelaos family has two members observed in the Sloan sample, one P- and one D-type, but this family has also been observed by F07 who identified it as the Anchises family. Analyzing the slopes provided by these authors together with the Sloan slopes, we conclude that 3 members are P-type –(1173), (23549), (24452)– and 3 members are D-type –(47967), (52511), 2001 SB173–. It is worth noting that the Sloan slope of (24452) is compatible with the slope published by F07.

### 4.2.2. Other families

Figure 15 shows the distributions of spectral slopes in terms of absolute magnitude of four L5 families: Aneas, Phereclos, 1988 RG10 and Asios.

The Aneas family has been studied by (Fornasier et al. 2004 - hereafter F04) and by F07, who treated it as the Sarpedon family. This family is actually formed from the merging of two families: Sarpedon and 1988 RN10. The Sarpedon family is resolved at  $d_{\text{cut}} < 130 \text{ m s}^{-1}$ , and the 1988 RN10 family is resolved at  $d_{\text{cut}} < 140 \text{ m s}^{-1}$ . Both families are identified down to  $d_{\text{cut}} = 90 \text{ m s}^{-1}$ . In Fig. 15a we show the spectral slopes of the whole Aneas family (i.e. Aneas + Sarpedon + 1988 RN10). The values indicate that this is a quite homogeneous D-type family, in agreement with F07<sup>6</sup>. The only two P-type members shown in Fig. 15a abandon the family at  $d_{\text{cut}} < 115 \text{ m s}^{-1}$ , so they are probably interlopers. So far, this family is one of the most homogeneous families in terms of taxonomy already detected, together with the Eurybates family in L4.

<sup>6</sup> Two members of the Sarpedon family observed by F07 –(48252) and (84709)–, that are not included in our Spectroscopic sample, are also classified as D-type.

The 1988 RG10 and the Asios families, shown in Figs. 15b,c, have not been observed before by spectroscopic surveys. The distribution of Sloan slopes indicates that the 1988 RG10 family would be a quite homogeneous D-type family. For the Asios family the results are inconclusive. The last family to be discussed here is the Phereclos family shown in Fig. 15d. It has been analyzed by F04 and F07 and their results point to a quite homogeneous D-type family. The only observation contained in the Sloan sample correspond to asteroid (18940), already observed by F04, and its Sloan slope is compatible with its Spectroscopic slope.

#### 4.3. Discussion

While the individual families in L5 appear to be taxonomically homogeneous, the individual families in L4 show a wide range of spectral slopes and a mixture of the C-, P- and D-types. There are, at least, two possibilities to explain the presence of different taxonomic classes within a single family:

- The family contains several interlopers, i.e. background asteroids that overlap with the family in proper elements. The amount of interlopers is significant because the presently observed family members are so sparse that we need to use large cutoff values to detect the family. Therefore, only the families detected at small cutoffs, like the Eurybates family, can be considered, for the time being, as the less contaminated by interlopers. Actually, the analysis of the Eurybates family made by F07 indicates that it would be the most homogeneous family of the Menelaus clan in terms of taxonomy. Note that the contamination by background interlopers would not introduce significant inhomogeneities in the taxonomy of L5 families, even if these families were not well defined, because most of these families are taxonomically indistinguishable from the background (in other words, the L5 families are dominated by D-type asteroids and the L5 background too).
- We may invoke some aging process on the surfaces of the asteroids, like the space weathering, that originates the wide range of slopes observed within a single family. In this case we must presume that the surfaces of the members of the family do not have the same age. In fact, many small members in the family may have been formed by secondary collisions, thus showing younger surfaces. Also, the small members, having a larger collision probability, may be more frequently affected by collisional resurfacing processes. Unfortunately, the space weathering is not well constrained in the case of the Trojan asteroids, and we cannot say whether it produces a reddening of the spectra with age, or viceversa (Moroz et al. 2004), or both. The lack of a clear correlation between spectral slope and size among the Trojan families, together with the still small amount of asteroids with known spectral slope and the poorly constrained collisional evolution of Trojan families, prevents to perform a reliable analysis of any aging process. Moreover, the apparent taxonomical homogeneity of the L5 families seems to play against the surface aging scenario.

Nevertheless, the case of the Eurybates/Menelaus families constitutes an interesting paradigm of the possible effect of space weathering on the surfaces of Trojan asteroids. The compactness of the Eurybates family, compared to the Menelaus family, may be interpreted as a rough measure of youthfulness. There are many examples in the Main Belt that support this idea: the

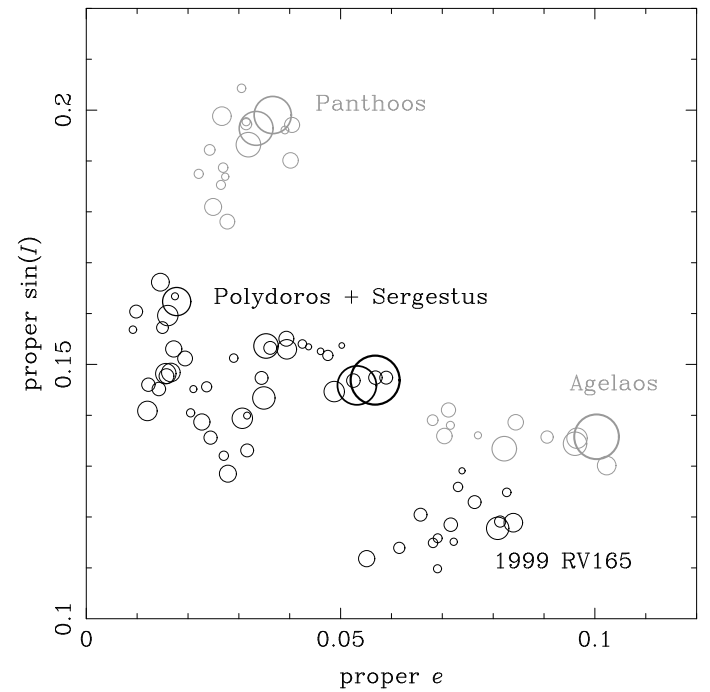


**Figure 13.** Distribution in the space of proper elements of the Anchises clan as detected at  $d_{\text{cut}} = 130 \text{ m s}^{-1}$ . It is constituted by five families: Panthoos, Polydoros, Sergestus, Agelaos and 1999 RV165. (1173) Anchises is incorporated to the Agelaos family at  $d_{\text{cut}} > 135 \text{ m s}^{-1}$ . The size of each circle is proportional to the asteroid size.

Karin family inside the Koronis family (Nesvorný et al. 2002), the Baptistina family inside the Flora clan (Bottke et al. 2007), and the Veritas family (Nesvorný et al. 2003). Within this hypothesis, the color distribution of the Eurybates/Menelaus families may be explained if we assume that the space weathering causes a reddening of the surfaces with age. Then, we may speculate that the members of the Eurybates family are the fresh fragments from the interior of a former member of the Menelaus family. The remaining members of the Menelaus family would have much older surfaces thus being much redder. An analysis of the family ages based on purely dynamical/collisional arguments is mandatory to better address this issue.

## 5. Conclusions

We have analyzed the distribution of spectral slopes and colors of Trojan asteroids using a sample of data from the SDSS-MOC3 together with a collection of spectra obtained from several surveys. Our analysis has been focused on the Trojan asteroid families. We have studied the global properties of the sample as well as the properties of some individual families. Our results can be summarized as follows:

- The analysis of photometric data from the SDSS-MOC3 produces reliable results that are comparable with those obtained from the analysis of spectroscopic data.
- The distribution of spectral slopes among the Trojan asteroids shows a clear bimodality. About 2/3 of the Trojan population is constituted by reddish objects that may be classified as D-type asteroids. The remaining bodies show less reddish colors compatible with the P-type, and only a small fraction (less than 10%) is constituted of bodies with neutral colors compatible with the C-type.

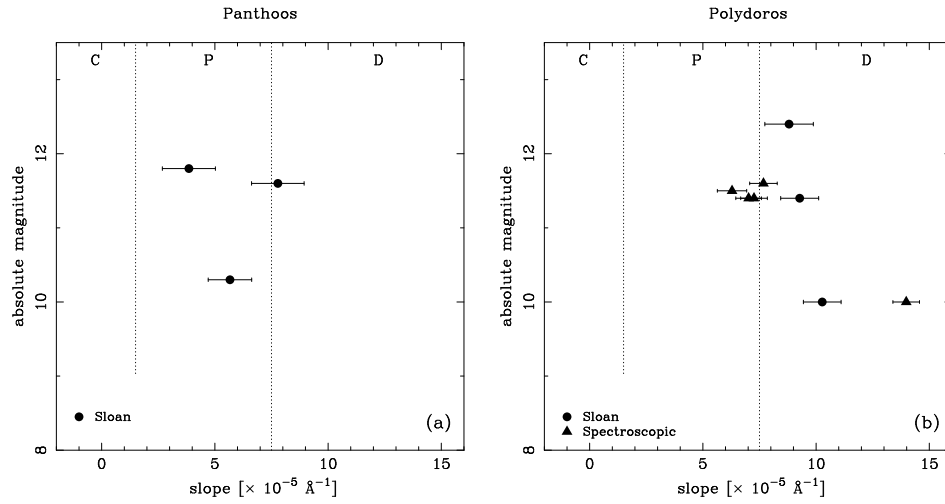


**Figure 14.** Distribution of Sloan slopes against absolute magnitude for three families of the Anchises clan: **(a)** Panthoos, **(b)** Polydoros and Sergestus. Full circles correspond to Sloan slopes. Triangles correspond to Spectroscopic slopes. The vertical dotted lines define the slope transition, within  $\pm 0.7 \times 10^{-5} \text{ \AA}^{-1}$ , between the different taxonomic classes indicate above the plots.

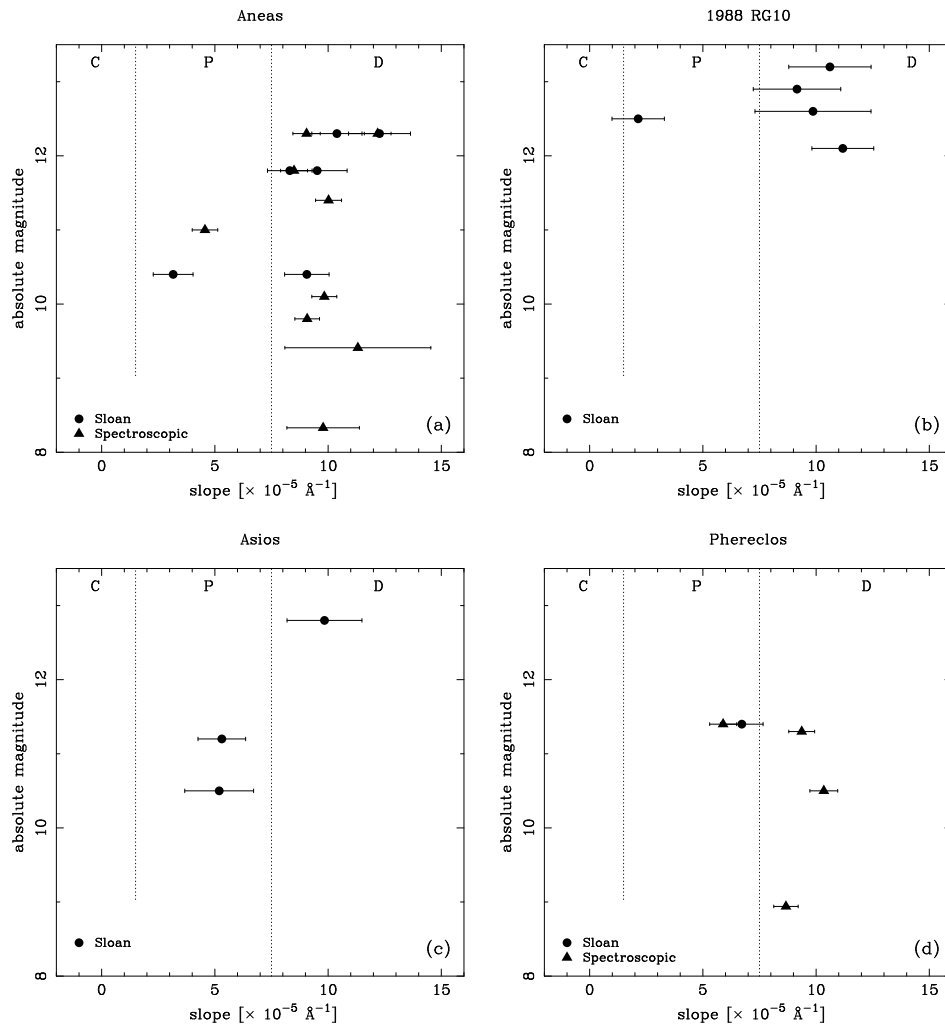


**Figure 15.** Same as Fig. 14 but for four different families in the L5 swarm.

- The members of asteroid families show a bimodal distribution with a very slight predominance of D-type asteroids. The background, on the contrary, is significantly dominated by D-type asteroids.
- The L4 and L5 swarms show significantly different distributions of spectral slopes. The distribution in L4 is bimodal with a slight predominance of D-type asteroids. The distribution in L5 is unimodal with a clear peak of D-type asteroids.

These differences can be attributed to the presence of asteroid families.

- The background asteroids show the same spectral slope distributions in both swarms, with a significant fraction ( $\sim 80\%$ ) of D-type asteroids. The families in L4 are dominated by P- and C-type asteroids, while the families in L5 are dominated by D-type asteroids.
- The background asteroids show correlations between spectral slope and orbital inclination and between spectral slope

and size. D-type asteroids dominate among the high inclination bodies and also among the large bodies. Low inclination bodies are slightly dominated by P-type asteroids. These correlations are most probably the result of the background collisional evolution, either by fragmentation or by collisional resurfacing. Similar correlations are not observed among the family members.

- Individual families in the L5 swarm are taxonomically homogeneous, but in the L4 swarm show a mixture of taxonomic types. This may be attributed to the presence of interlopers or to a surface aging effect.
- Any taxonomic analysis of individual families must be accompanied by a detailed analysis of the families structure as a function of the cutoff level of detection. An estimation of the family ages is also mandatory to complement these analysis.

*Acknowledgements.* We wish to thank Sonia Fornasier, Elisabetta Dotto, Phillippe Bendjoya and Alberto Cellino who kindly allowed us to use their spectroscopic data. Fruitful discussions with Jorge Carvano are also highly appreciated. This work has been supported by CNPq (Brazil) and SECYT (Argentina).

## References

- Beaugé, C. & Roig, F. 2001, *Icarus*, 153, 391
- Bendjoya, P., Cellino, A., di Martino, M., & Saba, L. 2004, *Icarus*, 168, 374
- Binzel, R. P., Masi, G., & Foglia, S. 2006, in *Bull. Amer. Astr. Soc.*, Vol. 38, 627
- Binzel, R. P., Masi, G., Foglia, S., et al. 2007, in *Lunar and Planetary Institute Conference Abstracts*, Vol. 38, 1851
- Botke, W., Vokrouhlický, D., & Nesvorný, D. 2007, in *AAS/Division for Planetary Sciences Meeting Abstracts*, Vol. 39, AAS/Division for Planetary Sciences Meeting Abstracts, #50.02
- Bus, S. J. & Binzel, R. P. 2002, *Icarus*, 158, 146
- Carvano, J. M., Mothé-Diniz, T., & Lazzaro, D. 2003, *Icarus*, 161, 356
- Dahlgren, M., Lagerkvist, C.-I., Fitzsimmons, A., Williams, I. P., & Gordon, M. 1997, *A&A*, 323, 606
- Dotto, E., Fornasier, S., Barucci, M. A., et al. 2006, *Icarus*, 183, 420
- Duffard, R. & Roig, F. 2007, *ArXiv e-prints*, 704
- Emery, J. P. & Brown, R. H. 2003, *Icarus*, 164, 104
- Fitzsimmons, A., Dahlgren, M., Lagerkvist, C. I., Magnusson, P., & Williams, I. P. 1994, *A&A*, 282, 634
- Fornasier, S., Dotto, E., Hainaut, O., et al. 2007, *Icarus*, 190, 622
- Fornasier, S., Dotto, E., Marzari, F., et al. 2004, *Icarus*, 172, 221
- Fukugita, M., Ichikawa, T., Gunn, J. E., et al. 1996, *AJ*, 111, 1748
- Gil-Hutton, R. & Brunini, A. 2007, *Icarus*, doi: 10.1016/j.icarus.2007.08.026
- Hammergren, M., Gyuk, G., & Puckett, A. W. 2007, in *Amer. Astr. Soc. Meeting Abstracts*, Vol. 210, #89.07
- Ivezić, Ž., Tabachnik, S., Rafikov, R., et al. 2001, *AJ*, 122, 2749
- Jewitt, D. C. & Luu, J. X. 1990, *AJ*, 100, 933
- Lazzaro, D., Angeli, C. A., Carvano, J. M., et al. 2004, *Icarus*, 172, 179
- Luu, J., Jewitt, D., & Cloutis, E. 1994, *Icarus*, 109, 133
- Marzari, F., Farinella, P., Davis, D. R., Scholl, H., & Campo Bagatin, A. 1997, *Icarus*, 125, 39
- Marzari, F. & Scholl, H. 1998, *A&A*, 339, 278
- Marzari, F., Scholl, H., & Farinella, P. 1996, *Icarus*, 119, 192
- Marzari, F., Tricarico, P., & Scholl, H. 2003, *MNRAS*, 345, 1091
- Milani, A. 1993, *Cel. Mech. Dyn. Astr.*, 57, 59
- Morbidelli, A., Levison, H. F., Tsiganis, K., & Gomes, R. 2005, *Nature*, 435, 462
- Moroz, M., Baratta, G., Strazzulla, G., et al. 2004, *Icarus*, 170, 214
- Nesvorný, D., Bottke, W. F., Levison, H. F., & Dones, L. 2003, *ApJ*, 591, 486
- Nesvorný, D., Bottke, Jr., W. F., Dones, L., & Levison, H. F. 2002, *Nature*, 417, 720
- Roig, F. & Gil-Hutton, R. 2006, *Icarus*, 183, 411
- Roig, F., Nesvorný, D., Gil-Hutton, R., & Lazzaro, D. 2007, *ArXiv e-prints*, 707
- Schwarz, R., Gyergyovits, M., & Dvorak, R. 2004, *Cel. Mech. Dyn. Astr.*, 90, 139
- Szabó, G. M., Ivezić, Ž., Jurić, M., & Lupton, R. 2007, *MNRAS*, 377, 1393
- Tholen, D. J. 1989, in *Asteroids II*, ed. R. P. Binzel, T. Gehrels, & M. S. Matthews (Univ. Arizona Press, Tucson, AZ), 1139–1150
- Xu, S., Binzel, R. P., Burbine, T. H., & Bus, S. J. 1995, *Icarus*, 115, 1
- Yang, B. & Jewitt, D. 2007, *AJ*, 134, 223
- Zappalà, V., Bendjoya, P., Cellino, A., Farinella, P., & Froeschlé, C. 1995, *Icarus*, 116, 291
- Zellner, B., Tholen, D. J., & Tedesco, E. F. 1985, *Icarus*, 61, 355

**Table 1.** Known Trojan asteroids included in our Sloan sample. The spectral slope  $S$  was computed by a linear fit to the  $g, r, i, z$  reflectance fluxes, normalized to 1 at the  $r$  band. For asteroids with two or more observations ( $N_{\text{obs}} > 1$ ), the table gives the average weighted slope of the observations. Family membership is indicated in the last column. Families were defined at a cutoff level of  $110 \text{ m s}^{-1}$  for the L4 swarm and  $120 \text{ m s}^{-1}$  for the L5 swarm.

L4 swarm					L5 swarm				
No.	Name	$S [\times 10^{-5} \text{ \AA}^{-1}]$	$N_{\text{obs}}$	Family	No.	Name	$S [\times 10^{-5} \text{ \AA}^{-1}]$	$N_{\text{obs}}$	Family
1749	Telamon	$8.69 \pm 0.75$	2	Menelaus	1870	Glaukos	$8.97 \pm 0.92$	1	
2260	Neoptolemus	$10.53 \pm 0.93$	1		1872	Helenos	$5.71 \pm 1.09$	2	
2759	Idomeneus	$9.82 \pm 0.82$	3		2674	Pandarus	$9.03 \pm 0.98$	1	
2797	Teucer	$9.32 \pm 1.03$	3	Teucer	3451	Mentor	$3.76 \pm 1.09$	3	
3564	Talthybius	$8.83 \pm 0.66$	1		3708	1974 FV1	$9.93 \pm 0.84$	1	
3793	Leonteus	$6.26 \pm 0.80$	1	Teucer	4792	Lykaon	$10.27 \pm 0.83$	1	Polydoros
4489	1988 AK	$10.49 \pm 0.68$	1		4827	Dares	$8.66 \pm 0.68$	1	
4946	Askalaphus	$9.31 \pm 0.88$	2		5257	1988 RS10	$12.18 \pm 1.68$	1	
5012	Eurymedon	$4.39 \pm 0.78$	1		5638	Deikoon	$7.32 \pm 0.95$	4	
5023	Agapenor	$4.70 \pm 0.45$	1	1986 WD	6997	Laomedon	$10.25 \pm 0.56$	1	
5025	1986 TS6	$5.18 \pm 0.87$	1	1986 TS6	11273	1988 RN11	$5.31 \pm 1.55$	1	
5027	Androgeos	$11.04 \pm 1.04$	1		11554	Asios	$5.19 \pm 1.52$	2	Asios
5028	Halaesus	$9.21 \pm 0.66$	1		11869	1989 TS2	$9.81 \pm 1.03$	4	
5259	Epeigeus	$11.39 \pm 0.74$	1		16560	1991 VZ5	$2.38 \pm 0.77$	4	
5264	Telephus	$10.90 \pm 0.56$	2		16667	1993 XM1	$9.26 \pm 0.94$	4	
5284	Orsilocus	$9.68 \pm 0.92$	1	Hektor	17414	1988 RN10	$10.39 \pm 1.11$	3	1988 RN10
6545	1986 TR6	$10.54 \pm 0.57$	1	1986 WD	17416	1988 RR10	$12.27 \pm 1.37$	1	Sarpedon
7214	Antielus	$4.77 \pm 0.79$	1	1986 WD	17419	1988 RH13	$3.16 \pm 0.88$	1	1988 RN10
8241	Agrius	$5.33 \pm 1.14$	1		17420	1988 RL13	$7.11 \pm 1.05$	3	1988 RL13
9590	1991 DK1	$7.38 \pm 0.87$	1		18046	1999 RN116	$10.19 \pm 0.72$	1	
9818	Eurymachos	$3.07 \pm 0.73$	1	Eurybates	18137	2000 OU30	$9.28 \pm 0.84$	2	Polydoros
10247	Amphiaraios	$6.23 \pm 1.38$	1	Kalchas	18940	2000 QV49	$6.72 \pm 0.94$	2	Phereclos
11396	1998 XZ77	$9.94 \pm 0.66$	1	1998 XZ77	19020	2000 SC6	$9.06 \pm 0.98$	4	1988 RN10
13331	1998 SU52	$4.05 \pm 1.22$	1	Demophon	19844	2000 ST317	$12.56 \pm 0.97$	1	
13362	1998 UQ16	$9.57 \pm 0.66$	1	Menelaus	24018	1999 RU134	$5.19 \pm 1.00$	2	
13387	Irus	$7.98 \pm 1.71$	1		24452	2000 QU167	$5.50 \pm 0.91$	1	Agelaos
13475	Orestes	$3.91 \pm 0.97$	1	Menelaus	24454	2000 QF198	$3.34 \pm 1.06$	1	
14235	1999 XA187	$9.92 \pm 1.11$	1		25347	1999 RQ116	$8.31 \pm 0.98$	2	Sarpedon
15536	2000 AG191	$9.96 \pm 0.83$	1		29314	1994 CR18	$4.16 \pm 1.13$	2	
15663	Periphas	$9.82 \pm 1.04$	2		30499	2000 QE169	$10.02 \pm 0.98$	1	2000 QE169
16152	1999 YN12	$4.98 \pm 0.99$	1		30505	2000 RW82	$11.51 \pm 1.01$	1	
18060	1999 XJ156	$4.83 \pm 1.01$	1	Eurybates	30705	Idaios	$9.84 \pm 0.80$	2	
18062	1999 XY187	$10.06 \pm 0.72$	1		30708	Echepolos	$8.58 \pm 1.11$	1	
19725	1999 WT4	$5.50 \pm 0.73$	1	Epeios	31814	1999 RW70	$11.18 \pm 1.37$	1	1988 RG10
20424	1998 VF30	$10.76 \pm 0.72$	2		32339	2000 QA88	$9.32 \pm 0.89$	2	
20995	1985 VY	$10.79 \pm 1.01$	3		32482	2000 ST354	$5.67 \pm 0.96$	1	Panthoos
21370	1997 TB28	$8.21 \pm 1.11$	1	Menelaus	32499	2000 YS11	$9.08 \pm 0.99$	7	
21599	1998 WA15	$8.88 \pm 0.96$	2	1998 XZ77	32811	Apisaon	$4.83 \pm 1.10$	1	
22049	1999 XW257	$5.15 \pm 1.14$	2		34298	2000 QH159	$8.11 \pm 1.33$	1	
22052	2000 AQ14	$6.27 \pm 1.45$	1	Epeios	38257	1999 RC13	$4.24 \pm 0.91$	1	
22404	1995 ME4	$4.04 \pm 0.98$	1		47969	2000 TG64	$9.52 \pm 1.32$	4	1988 RN10



Table 1. continued.

L4 swarm					L5 swarm				
No.	Name	$S$ [ $\times 10^{-5} \text{Å}^{-1}$ ]	$N_{\text{obs}}$	Family	No.	Name	$S$ [ $\times 10^{-5} \text{Å}^{-1}$ ]	$N_{\text{obs}}$	Family
23075	1999 XV83	$11.42 \pm 1.31$	1		48249	2001 SY345	$9.41 \pm 0.87$	1	
23123	2000 AU57	$7.58 \pm 0.79$	1	Epeios	51345	2000 QH137	$9.89 \pm 0.74$	1	
23144	2000 AY182	$5.82 \pm 0.81$	1	Epeios	51346	2000 QX158	$8.85 \pm 1.11$	1	
23285	2000 YH119	$10.81 \pm 0.62$	1		51364	2000 SU333	$6.33 \pm 1.07$	1	
23382	Epistrophos	$8.61 \pm 1.14$	2		51935	2001 QK134	$10.64 \pm 1.22$	1	
23706	1997 SY32	$6.46 \pm 1.32$	1	Menelaus	51994	2001 TJ58	$9.38 \pm 1.41$	2	
23939	1998 TV33	$5.21 \pm 0.53$	1		52273	1988 RQ10	$11.40 \pm 1.13$	1	
23963	1998 WY8	$2.52 \pm 1.08$	1	Kalchas	52511	1996 GH12	$11.86 \pm 1.10$	1	Agelaos
24225	1999 XV80	$4.64 \pm 0.99$	1	Epeios	52767	1998 MW41	$7.78 \pm 1.16$	3	Pantheoos
24233	1999 XD94	$4.71 \pm 0.98$	1	1986 WD	54596	2000 QD225	$2.14 \pm 1.16$	1	1988 RG10
24403	2000 AX193	$11.75 \pm 1.02$	1		55457	2001 TH133	$8.26 \pm 1.02$	2	
24426	2000 CR12	$5.58 \pm 1.46$	1	Eurybates	55460	2001 TW148	$6.06 \pm 1.48$	1	1999 RV165
24485	2000 YL102	$4.54 \pm 1.16$	1	1998 XZ77	55678	Lamos	$10.19 \pm 1.29$	1	
24498	2001 AC25	$3.05 \pm 1.37$	1	1986 TS6	56976	2000 SS161	$5.31 \pm 1.05$	1	Asios
24505	2001 BZ	$11.89 \pm 1.20$	1		57013	2000 TD39	$9.64 \pm 1.22$	1	2000 SA191
24508	2001 BL26	$5.29 \pm 1.25$	1	1999 XM78	57626	2001 TE165	$3.85 \pm 1.17$	1	Pantheoos
24539	2001 DP5	$8.04 \pm 1.15$	1		58008	2002 TW240	$7.53 \pm 2.93$	4	
24882	1996 RK30	$4.29 \pm 1.06$	2	Epeios	58084	Hiketaon	$9.87 \pm 1.27$	1	
31835	2000 BK16	$10.80 \pm 1.43$	2	1986 WD	62201	2000 SW54	$8.35 \pm 1.32$	1	
32498	2000 XX37	$10.70 \pm 0.88$	2		63955	2001 SP65	$11.31 \pm 1.23$	1	
33822	2000 AA231	$9.86 \pm 0.99$	1		64270	2001 TA197	$9.84 \pm 1.65$	2	Asios
35272	1996 RH10	$11.03 \pm 2.15$	2		65590	Archeptolemos	$6.58 \pm 1.29$	1	
36259	1999 XM74	$9.89 \pm 1.48$	1		73795	1995 FH8	$8.59 \pm 1.29$	1	
36279	2000 BQ5	$10.65 \pm 1.20$	2		76820	2000 RW105	$8.70 \pm 1.16$	2	
38052	1998 XA7	$2.87 \pm 1.39$	1		76824	2000 SA89	$6.87 \pm 1.49$	1	
38606	1999 YC13	$11.10 \pm 1.29$	1		76837	2000 SL316	$10.45 \pm 1.17$	1	
38614	2000 AA113	$5.32 \pm 1.05$	1	Sinon	77891	2001 SM232	$6.60 \pm 1.54$	1	
38617	2000 AY161	$3.85 \pm 1.00$	1	1986 TS6		1988 SJ2	$12.80 \pm 1.43$	1	
38619	2000 AW183	$8.25 \pm 1.31$	1			2000 QZ75	$10.37 \pm 1.48$	2	
38621	2000 AG201	$5.89 \pm 1.21$	1			2000 RE29	$11.37 \pm 1.44$	1	Deiphobus
39264	2000 YQ139	$11.64 \pm 1.34$	1	Hektor		2000 SG187	$5.01 \pm 1.16$	1	
39287	2001 CD14	$3.87 \pm 1.72$	1	Laertes		2000 SK47	$9.06 \pm 1.56$	4	
39293	2001 DQ10	$9.13 \pm 1.31$	1	1986 WD		2000 SM250	$11.08 \pm 1.45$	1	
41268	1999 XO64	$10.00 \pm 1.19$	2			2000 SP92	$10.25 \pm 1.44$	1	2000 RO85
42168	2001 CT13	$3.28 \pm 0.98$	1			2000 SR79	$8.81 \pm 1.07$	1	Sergestus
42179	2001 CP25	$4.19 \pm 1.26$	1	Kalchas		2000 SZ135	$9.12 \pm 0.93$	2	
42403	Andraimon	$6.49 \pm 1.18$	1			2000 TU44	$8.92 \pm 1.17$	2	
43212	2000 AL113	$1.12 \pm 0.89$	1	Eurybates		2001 QM257	$8.89 \pm 1.10$	1	
43706	Iphiklos	$5.56 \pm 1.17$	1	Makhaon		2001 RN122	$10.02 \pm 1.94$	1	1988 RL13
51378	2001 AT33	$9.74 \pm 0.97$	1			2001 SA220	$13.07 \pm 1.88$	1	1988 RG10
53477	2000 AA54	$6.24 \pm 0.87$	1	1986 WD		2001 SC101	$9.86 \pm 2.56$	2	1988 RG10
55568	2002 CU15	$12.53 \pm 1.29$	1			2001 SC137	$9.16 \pm 1.93$	1	1988 RG10
55571	2002 CP82	$4.70 \pm 0.98$	1			2001 SD30	$9.98 \pm 1.49$	1	2000 SA191

Table 1. continued.

L4 swarm					L5 swarm				
No.	Name	$S [\times 10^{-5} \text{\AA}^{-1}]$	$N_{\text{obs}}$	Family	No.	Name	$S [\times 10^{-5} \text{\AA}^{-1}]$	$N_{\text{obs}}$	Family
57920	2002 EL153	$8.80 \pm 1.31$	1	Laertes	2001 TK131	$8.98 \pm 1.68$	2		
58473	1996 RN7	$4.85 \pm 1.32$	1		2001 TO108	$9.70 \pm 1.12$	1		
58479	1996 RJ29	$6.41 \pm 1.28$	1	Menelaus	2001 VB52	$10.83 \pm 1.56$	1	2000 SY317	
60383	2000 AR184	$10.42 \pm 0.80$	1		2001 WX20	$5.07 \pm 1.66$	1		
63202	2000 YR131	$4.24 \pm 0.98$	1	1999 XM78	2001 XV105	$8.74 \pm 1.67$	2		
63210	2001 AH13	$11.28 \pm 1.20$	1	1986 TS6	2002 VH107	$8.83 \pm 1.24$	2	Bitias	
63257	2001 BJ79	$4.74 \pm 1.32$	1	Euryalos	2003 WQ25	$10.61 \pm 1.82$	1	1988 RG10	
63259	2001 BS81	$5.44 \pm 1.74$	2	Demophon					
63265	2001 CP12	$10.27 \pm 1.31$	1						
63272	2001 CC49	$7.71 \pm 1.52$	1						
63286	2001 DZ68	$7.15 \pm 1.32$	1						
63291	2001 DU87	$5.96 \pm 1.31$	1	Menelaus					
63292	2001 DQ89	$3.99 \pm 1.29$	1						
63294	2001 DQ90	$11.57 \pm 1.55$	3						
65000	2002 AV63	$8.47 \pm 1.70$	2	Hektor					
65134	2002 CH96	$2.45 \pm 1.07$	1						
65194	2002 CV264	$10.45 \pm 2.06$	2						
65209	2002 DB17	$9.94 \pm 1.26$	1	Sinon					
65224	2002 EJ44	$5.38 \pm 2.01$	1						
65225	2002 EK44	$2.56 \pm 1.43$	1	Eurybates					
65583	Theoklymenos	$7.93 \pm 1.34$	1	Menelaus					
79444	1997 UM26	$5.77 \pm 1.31$	2						
80302	1999 XC64	$8.14 \pm 1.71$	1	Sinon					
83975	2002 AD184	$5.78 \pm 1.25$	1						
83977	2002 CE89	$5.17 \pm 1.33$	1	Menelaus					
83983	2002 GE39	$8.81 \pm 1.57$	1						
88225	2001 BN27	$13.72 \pm 1.35$	1						
89829	2002 BQ29	$5.84 \pm 1.07$	1						
89871	2002 CU143	$10.72 \pm 1.39$	2	Epeios					
89924	2002 ED51	$9.47 \pm 1.37$	2	1999 XM78					
	1995 QC6	$4.20 \pm 1.14$	1						
	1996 TA58	$10.55 \pm 1.55$	1						
	1997 WA12	$8.97 \pm 1.42$	1						
	1999 XJ55	$11.88 \pm 1.74$	1						
	2000 AG90	$11.98 \pm 1.55$	1	Sinon					
	2000 AJ114	$10.26 \pm 1.18$	1	Makhaon					
	2000 AL8	$11.27 \pm 1.75$	1						
	2000 BV1	$4.41 \pm 1.38$	1						
	2000 YB131	$10.92 \pm 1.31$	3						
	2000 YC112	$7.30 \pm 1.35$	4	1998 XZ77					
	2000 YS109	$4.39 \pm 1.14$	1	1998 XZ77					
	2001 AG51	$5.20 \pm 1.47$	1	Laertes					
	2001 BD49	$11.43 \pm 1.23$	1						

Table 1. continued.

L4 swarm					L5 swarm				
No.	Name	$S [\times 10^{-5} \text{\AA}^{-1}]$	$N_{\text{obs}}$	Family	No.	Name	$S [\times 10^{-5} \text{\AA}^{-1}]$	$N_{\text{obs}}$	Family
	2001 BS16	$10.01 \pm 1.73$	2						
	2001 DL10	$9.42 \pm 1.31$	1						
	2001 DO93	$12.87 \pm 1.86$	2						
	2001 FV58	$12.96 \pm 1.52$	1	Epeios					
	2002 AE166	$0.95 \pm 1.36$	1	Eurybates					
	2002 CH109	$6.64 \pm 1.69$	1	Epeios					
	2002 CL109	$6.49 \pm 1.51$	2	1998 US24					
	2002 CL130	$6.26 \pm 1.17$	1	Laertes					
	2002 CN130	$9.79 \pm 1.10$	1						
	2002 CQ186	$6.37 \pm 1.91$	1	Laertes					
	2002 CZ256	$2.26 \pm 1.53$	2	Menelaus					
	2002 DD1	$10.77 \pm 1.67$	2						
	2002 DW15	$9.43 \pm 1.61$	2	Hektor					
	2002 DX12	$8.50 \pm 1.25$	1	Euryalos					
	2002 EK51	$12.10 \pm 1.77$	1						
	2002 EP106	$3.16 \pm 1.35$	1						
	2002 ES83	$10.29 \pm 1.66$	2						
	2002 ET136	$8.99 \pm 1.54$	1						
	2002 EU14	$6.52 \pm 2.69$	2						
	2002 EX5	$2.84 \pm 1.64$	1	Epeios					
	2002 FL37	$5.32 \pm 1.70$	1						
	2002 FM7	$12.12 \pm 2.42$	1						
	2002 GG33	$13.05 \pm 1.27$	1	Menelaus					
	2002 GO150	$1.75 \pm 1.68$	1	Demophon					
	2003 FJ64	$7.01 \pm 1.29$	1	Menelaus					
	2003 FR72	$5.83 \pm 1.59$	1	Hektor					
	2003 GU35	$7.95 \pm 1.54$	1						
	2003 GX7	$11.87 \pm 1.41$	1						
	2004 HS1	$7.60 \pm 1.45$	1						
	2004 JO43	$4.69 \pm 1.76$	1						
	2004 KJ4	$7.35 \pm 1.15$	1	Menelaus					
	5214 T-2	$7.42 \pm 1.11$	1	Euryalos					

**Table 2.** Trojan asteroids included in our Spectroscopic sample. The spectral slope  $S$  was computed by a linear fit, in the interval 5000–9200 Å, of the rebinned spectra normalized to 1 at 6240 Å. For asteroids with more than one observation ( $N_{\text{obs}} > 1$ ), the table gives the average weighted slope of the observations. We recall that different observations of the same asteroid come from different surveys. Family membership is indicated in the last column. Families were defined at a cutoff level of 110 m s<sup>-1</sup> for the L4 swarm and 120 m s<sup>-1</sup> for the L5 swarm.

L4 swarm					L5 swarm				
No.	Name	$S$ [ $\times 10^{-5} \text{Å}^{-1}$ ]	$N_{\text{obs}}$	Family	No.	Name	$S$ [ $\times 10^{-5} \text{Å}^{-1}$ ]	$N_{\text{obs}}$	Family
588	Achilles	$2.09 \pm 0.64$	1		1172	Aeneas	$9.78 \pm 1.60$	2	Aeneas
911	Agamemnon	$9.12 \pm 4.14$	2		1871	Astyanax	$5.45 \pm 0.56$	1	
1143	Odysseus	$11.07 \pm 0.63$	1		2223	Sarpedon	$11.31 \pm 3.22$	2	Sarpedon
1647	Menelaus	$6.62 \pm 0.53$	1	Menelaus	2357	Phereclos	$8.67 \pm 0.54$	1	Phereclos
1749	Telamon	$10.08 \pm 0.62$	1	Menelaus	2895	Memnon	$-1.59 \pm 0.72$	1	
1868	Thersites	$8.78 \pm 0.60$	1		3317	Paris	$7.94 \pm 3.70$	2	
2920	Automedon	$10.34 \pm 0.59$	1		3451	Mentor	$1.40 \pm 0.57$	1	
3063	Makhaon	$8.33 \pm 0.52$	1	Makhaon	3708	1974 FV1	$8.60 \pm 0.53$	1	
3709	Polypoites	$11.19 \pm 0.62$	2		4348	Poulydamas	$4.12 \pm 0.53$	1	
3793	Leonteus	$7.67 \pm 0.54$	1	Teucer	4715	1989 TS1	$14.61 \pm 0.59$	1	
4035	1986 WD	$12.42 \pm 1.91$	2	1986 WD	4792	Lykaon	$13.98 \pm 0.59$	1	Polydoros
4060	Deipylos	$1.75 \pm 2.46$	2		5130	Ilioneus	$9.08 \pm 0.54$	1	Sarpedon
4063	Euforbo	$8.28 \pm 0.55$	2		5511	Cloanthus	$13.27 \pm 0.57$	1	Cloanthus
4068	Menestheus	$10.77 \pm 1.61$	2		5648	1990 VU1	$10.46 \pm 2.35$	2	
4138	Kalchas	$6.53 \pm 0.65$	1	Kalchas	6998	Tithonus	$9.36 \pm 0.57$	1	Phereclos
4489	1988 AK	$8.55 \pm 0.54$	1		7352	1994 CO	$6.46 \pm 3.52$	2	1994 CO
4833	Meges	$10.90 \pm 0.54$	2		9430	Erichthonios	$10.34 \pm 0.62$	1	Phereclos
4834	Thoas	$11.01 \pm 0.54$	1		11089	1994 CS8	$3.96 \pm 0.55$	1	Anchises
4835	1989 BQ	$5.89 \pm 3.39$	2		15502	1999 NV27	$9.83 \pm 0.55$	1	Aeneas
4836	Medon	$8.80 \pm 0.55$	1		15977	1998 MA11	$7.50 \pm 0.57$	1	1998 MA11
4902	Thessandrus	$8.30 \pm 0.54$	1		17416	1988 RR10	$9.05 \pm 0.60$	1	Sarpedon
5025	1986 TS6	$15.36 \pm 0.71$	1	1986 TS6	18137	2000 OU30	$7.26 \pm 0.59$	1	Polydoros
5126	Achaemenides	$0.76 \pm 0.53$	1		18268	Dardanos	$12.19 \pm 0.59$	1	Sarpedon
5244	Amphilochos	$2.94 \pm 0.53$	1	Menelaus	18493	1996 HV9	$4.56 \pm 0.56$	2	Sarpedon
5254	Ulysses	$9.99 \pm 0.52$	1		18940	2000 QV49	$5.89 \pm 0.59$	1	Phereclos
5258	1989 AU1	$7.48 \pm 0.53$	1	Menelaus	23694	1997 KZ3	$7.02 \pm 0.56$	1	Sergestus
5264	Telephus	$11.68 \pm 1.05$	2		24467	2000 SS165	$10.02 \pm 0.57$	1	Sarpedon
5283	Pyrrhus	$-6.58 \pm 0.56$	1		25347	1999 RQ116	$8.50 \pm 0.59$	1	Sarpedon
5285	Krethon	$6.53 \pm 0.59$	1		30698	Hippokoon	$7.68 \pm 0.61$	1	Sergestus
6090	1989 DJ	$12.54 \pm 0.64$	1		32430	2000 RQ83	$6.29 \pm 0.65$	1	Sergestus
6545	1986 TR6	$9.15 \pm 0.53$	1	1986 WD	32615	2001 QU277	$8.34 \pm 0.57$	1	
7152	Euneus	$5.61 \pm 0.61$	1	Euneus	34785	2001 RG87	$2.58 \pm 0.59$	1	
7641	1986 TT6	$4.66 \pm 0.66$	1		48249	2001 SY345	$9.60 \pm 0.60$	1	
11351	1997 TS25	$9.10 \pm 0.56$	1	1986 WD					
12917	1998 TG16	$11.19 \pm 0.57$	1	1986 TS6					
12921	1998 WZ5	$4.05 \pm 0.54$	1	1986 TS6					
13463	Antiphos	$4.75 \pm 0.76$	2	1986 TS6					
15094	1999 WB2	$2.59 \pm 0.55$	1						
15535	2000 AT177	$10.92 \pm 0.56$	2	1986 TS6					
20738	1999 XG191	$9.70 \pm 0.56$	1	1986 TS6					
24390	2000 AD177	$9.74 \pm 0.54$	1	1986 TS6					